



**MULTISCALE MODELLING OF BIOGAS
PURIFICATION USING MONTMORILLONITE
ADSORBENT**

**Submitted in fulfillment of the requirements for the degree of:
Master of Engineering in the Department of Chemical Engineering,**

Faculty of Engineering and the Built Environment

at Durban University of Technology

By

Thandeka Ntombifuthi Khuzwayo (21960130)

Date: March 2024

Supervisor: Dr P. T Ngema /Prof. S Ramsuroop / Dr M. M Lasich

PREFACE

I was registered at Durban University of Technology, doing this work from August 2021 to January 2024 under the supervision of Dr P.T. Ngema, Dr M. Lasich and Prof S. Ramsuroop. This work is original.

Student: Ntombifuthi Thandeka Khuzwayo

Signature...

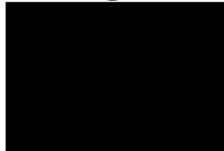


Date: 18/03/2024

As the candidate's supervisor, I agree to the submission of this dissertation/thesis.

Supervisor: Dr PT Ngema.

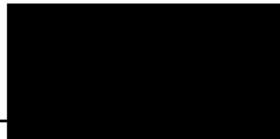
Signature...



Date: 22/03/24

Co-Supervisor: Dr MM Lasich

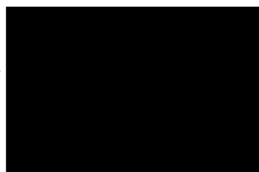
Signature..



Date: 22/03/24

Co-Supervisor: Prof S Ramsuroop

Signature...



Date: 22/03/24

DECLARATION

I, the undersigned Ntombifuthi Thandeka Khuzwayo (21960130) declares this research titled: Multiscale Modelling of Biogas Purification using Montmorillonite adsorbent was accomplished by myself and it has not been submitted in any other institute or university for a degree.

This dissertation/thesis does not contain other persons' writing, unless specifically acknowledged as being sourced from other researchers. Where other written sources have been quoted, then their words have been re-written, but the general information attributed to them has been referenced.

Unless otherwise noted when the source is cited in the dissertation/thesis and References sections, no text, graphics, or tables from the Internet have been copied and pasted into this work.

Signed:



ACKNOWLEDGEMENT

I would like to acknowledge the following individuals and institutions.

- I am deeply thankful to the Almighty for giving me the opportunity and determination to complete my research.
- The Department of Chemical Engineering at DUT for offering the author and opportunity of doing this research.
- To my supervisors Dr P.Thokozani Ngema and Prof Suresh Ramsuroop I am truly honoured for their unwavering support, guidance and skills to carry out this research.
- Dr Madison Lasich for all the advice and assistance on the topic simulation topic, and also guiding me through the entire project.
- To share my gratitude towards Sapref supporting me financially.
- My fellow postgraduates and colleagues for their guidance and support whenever I was in need. And also give thanks to my family for giving me courage and support all till the end of my research.
- To the Center of High-Performance Computer (CHPC) I high appreciate the training and the time provided for me to carry out my simulation analyses for the duration of my work.

ABSTRACT

Biogas, a renewable energy source derived from organic materials, offers significant potential for creating sustainable power sources and minimize environmental pollution. However, the presence of contaminants like carbon dioxide (CO₂) and hydrogen sulfide (H₂S) in biogas can reduce its usefulness and efficiency in a number of applications. To address this issue, this research focuses on the purification of biogas using clay adsorbent.

This study investigates the adsorption capacity of clay minerals, such as montmorillonite, in removing CO₂ and H₂S from biogas. In this study, Grand Canonical Monte Carlo (GCMC) simulations were performed using a self-consistent forcefield to predict adsorption isotherms for methane, carbon dioxide, ethane, and hydrogen sulfide in montmorillonite lattice. The experimental setup involved a Pressure Swing Adsorption (PSA) column, where biogas passes through the adsorbent, leading to the adsorption of impurities while maintaining the methane content, thus enhancing the overall biogas quality.

The model was fitted with Langmuir adsorption isotherms for all species at different pressures and ambient temperature, coupled with batch equilibrium approach to model the PSA system. The equilibrium modelling of a pressure swing adsorption system to purify CH₄/CO₂ feedstock was demonstrated in such that a system can be incorporated into a solar biogas reforming process, targeting purity of 93-96 mol-% methane, which was readily achievable.

The modelling of PSA indicate that the system could produce over 96% of methane and a recovery of around 82% at low pressure. The findings suggest that the choice of clay adsorbent and optimization of process parameters can significantly enhance the purification efficiency of biogas via pressure-swing adsorption. The strong selectivity of the montmorillonite adsorbent has affinity to adsorb carbon dioxide and other species at low pressures, even though nitrogen require more pressure to be adsorbed onto the montmorillonite bed.

TABLE OF CONTENT

PREFACE	ii
DECLARATION	iii
ACKNOWLEDGEMENT	iv
ABSTRACT.....	v
TABLE OF CONTENT	vi
LIST OF FIGURES.....	x
LIST OF TABLES	xii
NOMENCLATURE.....	xiv
1 CHAPTER 1-INTRODUCTION	1
1.1 Background.....	1
1.2 Problem statement.....	2
1.3 Aims and objectives.....	3
1.4 Approach.....	4
1.5 Structure of the thesis	5
2 CHAPTER 2- LITERATURE REVIEW	6
2.1. Introduction.....	6

2.2.	Montmorillonite	6
2.3.	Biogas	7
2.3.1.	Biogas Plants	9
2.4.	Biogas Industry in South Africa	10
2.4.1.	Access to clean Renewable Energy	11
2.5.	Biogas Production.....	13
2.6.	Biogas Upgrading	14
2.6.1.	Biogas Upgrading Technologies	15
2.6.2.	Physical /Chemical Scrubbing	17
2.6.3.	Membrane Technology.....	18
2.6.4.	Cryogenic Separation	20
2.7.	Pressure Swing Adsorption (PSA).....	22
2.7.1.	Principles of Pressure Swing Adsorption	23
2.8.	Literature Survey on Research Performed to upgrade Biogas quality.....	24
2.9.	Previous studies	28
2.10.	Biogas upgrade technology limitations.....	33
3	CHAPTER 3-MATERIALS AND METHODS.....	34
3.1.	Introduction.....	34

3.2.	Montmorillonite	34
3.3.	Grand Canonical Monte Carlo Simulation	36
3.4.	Simulation Details.....	36
3.5.	Adsorption Isotherms.....	39
3.6.	Batch Equilibrium Modelling	41
4	CHAPTER 4- RESULTS AND DISCUSSIONS.....	42
4.1.	Introduction.....	42
4.2.	Results.....	42
4.3.	Discussion.....	42
4.4.	Batch Equilibrium Modelling	49
5	CHAPTER 5-CONCLUSIONs and RECOMMENDATIONS	53
5.1.	Conclusion	53
5.2.	Recommendations.....	55
6	REFERENCES.....	56
A.	APPENDIX A: Simulation details and calculations	62
B.	APPENDIX B: Calculations for Best fit Model.....	68
	B1: Comparison between Langmuir, Freundlich and Redlich -Peterson using the following equations respectively:	68

C.	APPENDIX C: Operating conditions for psa system.....	75
C.1.	Best Operating Condition for PSA System.....	75

LIST OF FIGURES

Figure 1-1 Analysis of diverse carbon dioxide discharges linked to various alternatives of power generation	8
Figure 2-2 Illustration of biogas plants in Europe per country in 2015	10
Figure 2-3 Biogas production via anaerobic digestion	13
Figure 2-4 Water Scrubbing Technology	16
Figure 2-5 Biogas upgrading by chemical absorption amine scrubbing	18
Figure 2-5 Two Stage Membrane Process Biogas Upgrading process	19
Figure 2-6 Biogas upgrading procedure by cryogenic separation.....	21
Figure 2-7: CO ₂ , CH ₄ , N ₂ adsorption at low pressure from 0 to 10 Bar and 298K	29
Figure 2-8: Adsorption isotherms for the components between MMT1-MMT at 50 bar and, 298 and 323 K	30
Figure 2-9: Thermal gravimetric analysis of nano modified and amino modified clay	31
Figure 3-1 Structure of montmorillonite generated using Material Studio Software.....	35
Figure 4-1 Amount of gas adsorbed into the solid q and fugacity f of the gas.	46
Figure 4-2: Heat map of the overall biogas component in the outlet stream of PSA system as a function of adsorbent quantity and operating pressure ratio.	50
Figure 4-3 Heat map of the overall biogas component in the outlet stream of PSA system as a function of adsorbent quantity and operating pressure ratio.	51

Figure A-1 The flow diagram for co-precipitation method used to synthesize magnetite.....	65
Figure A-2 The quantity of gas adsorbed into the adsorbent q , and P as the pressure.....	65
Figure A-4 The quantity of gas adsorbed into the adsorbent q , and P as the pressure.....	66
Figure A-5 The quantity of gas adsorbed into the adsorbent q , and P as the pressure.....	67
Figure C-1 Generated results obtained for PSA system using Octave tool.....	75

LIST OF TABLES

Table 2-1 Physical properties and BET Analysis of Nano clays materials.....	32
Table 3-1 Feed composition and simulation parameters.....	41
Table 4-1 Adsorption isotherm for CH ₄ at 298K and 1.0 x10 ⁻³ to 1.0 x10 ³ kPa.....	43
Table 4-2 Adsorption isotherm for C ₂ H ₆ at 298K and 1.0 x10 ⁻³ to 1.0 x10 ³ kPa.	43
Table 4-3 Adsorption isotherm for N ₂ at 298K and 1.0 x10 ⁻³ to 1.0 x10 ³ kPa.	44
Table 4-4 Adsorption isotherm for CO ₂ at 298K and 1.0 x10 ⁻³ to 1.0 x10 ³ kPa.....	44
Table 4-5 Adsorption isotherm for H ₂ S at 298K and 1.0 x10 ⁻³ to 1.0 x10 ³ kPa.....	45
Table 4-6 Fitted Langmuir Adsorption Mode Parameters Q _o along with the Sum-Square Error (SSE) and the Correlation Coefficient (R ²).....	47
Table 4-7 Fitted Freundlich Adsorption Mode Parameters and K along with the Sum-Square Error (SSE) and the Correlation Coefficient (R ²).....	47
Table 4-8 Fitted Redlich -Peterson Adsorption Mode Parameters aR, Bs, Kg and the Correlation Coefficient (R ²)	48
Table 4-9 Comparison between different fitted models of Biogas species.	48
Table 4-10 Overall bed mass (W) of the PSA system at 298K and 101.325kPa	50
Table A-1 Present calculations pf standard deviation	62
Table A-2 Present calculations pf standard deviation	62

Table A-3 Present calculations pf standard deviation	63
Table A-4 Present calculations pf standard deviation	64
Table A-5 Present calculations pf standard deviation	64
Table B-1 CH ₄ Fitted Mode parameters of Langmuir, Freundlich and Redlich-Peterson along with RMSE and R ²	70
Table B-2 C ₂ H ₆ Fitted Mode parameters of Langmuir, Freundlich and Redlich-Peterson along with RMSE and R ²	71
Table B-3 CO ₂ Fitted Mode parameters of Langmuir, Freundlich and Redlich-Peterson along with RMSE and R ²	72
Table B-4 H ₂ S Fitted Mode parameters of Langmuir, Freundlich and Redlich-Peterson along with RMSE and R ²	73
Table B-5 N ₂ Fitted Mode parameters of Langmuir, Freundlich and Redlich-Peterson along with RMSE and R ²	74
Table C-1 Number of moles for the inlet stream.....	76
Table C-1 Number of moles for the inlet stream.....	76
Table C-3 Bed size for CH ₄ outlet stream.....	77

NOMENCLATURE

A	Bond Angle
AC	Activated Carbon
Al	Aluminum
APTMS	aminopropyltrimethoxysilane
BET	Brunauer–Emmett–Teller
CO ₂	Carbon Dioxide
CH ₄	Methane
CME	Clay Modified Electrodes
CMS	Carbon Molecular Sieve
GHG	Green House Gases
CHP	Combined Heat and Power
CHPC	Center of High-Performance Computing
DDA	dimethyl-dialkyl amine
Fe	Iron
GCMC	Grand Canonical Monte Carlo
GNU	G Octave Unit
H ₂ S	Hydrogen Dioxide
IAST	Ideal Adsorption Solution Theory
K _f	Freundlich Constant

KOH	Potassium hydroxide
kPa	Kilo Pascal
KW	Killo Watts
MWh	Mega Watts per hour
MMT	Montmorillonite
MTZ	Mass Transfer Zone
N ₂	Nitrogen
ODA	octadecyl-amine
NaOH	Sodium hydroxide
PSA	Pressure Swing Adsorption
R ²	Correlation Coefficient
RE	Renewable Energy
RMSE	Root Mean Square Error
Si	Silicon
SSE	Sum Square Error
TD	Digester Temperature
VOC	Volatile Organic Compound
VPSA	Vacuum Pressure Swing Adsorption

CHAPTER 1-INTRODUCTION

1.1 Background

With the current energy crisis in South Africa, biogas should be explored and exploited more as an alternative and complementary energy source. However, to increase biogas production, there are still some vital processes that need to be improved, for environmental and economic reasons. The use of this variant of green energy source would decrease the nation's dependency on depleting fossil fuels which are large contributors to rise of the level of CO₂ and its impacts. The current consumption of fossil fuels, as well as the environmental impact of greenhouse gases, are driving research into renewable energy production from organic resources and waste.

However, the biogas industry in South Africa is still in its infancy, even though the first biogas implementations in South Africa began in 1962 but failed to progress for unclear reasons(Thopil et al., 2018). In developed nations such Germany, Austria, and Sweden, however, the biogas industry did mature(Ingo et al., 2022). Unfortunately, biogas production has also historically been documented to produce some greenhouse gases, namely, methane (CH₄) and carbon dioxide (CO₂). Biogas purification studies have thus been undertaken to reduce the emissions it releases to the environment.

There are five essentials renewable energy sources (RE): solar energy, hydropower, wind energy, biomass energy, and geothermal energy that are used around the globe. These resources have a vital chance of helping many nations deal with the current energy crisis. Therefore, maintaining these assets' improvement is crucial to resolving the current energy challenges(Abdul et al., 2022). Remarkably, the majority of research on renewable energy has been carried out in rich countries with steady energy supplies. As a result, making sure that such climate-friendly technology is widely deployed is a crucial concern for developing nations(Koniuszewska et al., 2021). Investment in RE technology, like solar photovoltaic panels, has already resulted in substantial cost savings in several economies, as they do not require fuel which needs to be extracted and transported. To meet their energy needs, the majority of nations have diversified into various renewable and sustainable energy sources. These changes include detrimental effects on health, the environment, and the potential depletion of fossil fuels (oil, gas, and coal) and/or low water table, which is what causes the decline in dam water levels(Gielen et al., 2019). The following sections include an overview of the possible reserves of solar, wind, hydropower, and biomass resources. Such technologies have a tremendous capacity for countries. Examples include

Pakistan, China, Germany, India, Brazil, USA, which has already introduced many of the RE technologies that have been discussed. The most widely used RE technologies are Hydropower and Solar power which ideally used for industrial energy supply.

1.2 Problem statement

Because of its economic and environmental sustainability, the ongoing global shift in the energy sector from fossil fuels to low-carbon sources has been progressively integrated into national energy plans(Kihombo et al., 2021). Biogas preserves 75 to 80% of its energy content and can be used in power generation, although raw biogas sources (whether from landfill or anaerobic digestion) lead to a diverse range of impurities which contribute towards climate change around the globe(Rafiee et al., 2021).

Renewable energy sources (RE) offer an alternative solution to non-sustainable energy sources and reduce economic cost, environmental impact and improve social welfare. Although selection of RE resources have a high preference, from the technical aspects, the maturity of the technology is essential for the implementation of RE sources. In terms of environmental, land requirement CO₂ emitted during biogas combustion is part of the natural carbon cycle since the organic materials used to produce biogas initially absorbed CO₂ during their growth(Damyanova and Beschkov, 2020). By capturing and utilizing biogas, methane emissions from waste decomposition are significantly reduced, contributing to climate change mitigation. Biogas purification studies have been undertaken in the direction of reducing the emissions released to the environment, however each technology comes with its own unique limitations and sensitivity to contaminants, such as selectivity of the adsorbent that would produce high purity of the upgraded biogas. Some technology requires intensive-energy processes to remove impurities like CO₂ and moisture form biogas (Das et al., 2022) .

This study would explore the differential sorption of the various gases in pressure swing operation to separate the various components for downstream processing. The main aim is to investigate the suitability of montmorillonite as a novel adsorbent for biogas purification. This will be accomplished by using Monte Carlo simulations in the grand canonical ensemble simulation to develop adsorption isotherms, along with macro-scale batch equilibrium modeling.

1.3 Aims and objectives.

In many gas separation applications, the Pressure Swing Adsorption (PSA) optimization procedures provide realistic statistical information based on historical and empirical data through the design of experiment techniques. It is anticipated that the competitiveness of this technique for upgrading biogas would increase. The main focus of this study is:

- To determine the effectiveness of montmorillonite as a biogas purifier. Montmorillonite has shown promise as a biogas purifier due to its high surface area and ion exchange capacity. These properties make it effective in adsorbing and removing H₂S from biogas to an acceptable level. Other impurities such as ammonia, nitrogen, propane, and ethane may be present in the biogas, and the choice of purification process is determined by the specific pollutants present as well as the biogas's intended purpose. The study focuses more on the removal of carbon dioxide and hydrogen sulphide.
- Establish the optimal operating condition of a Pressure Swing Adsorption (PSA) system using montmorillonite. The main cause of this is the degree of complexity that a PSA displays in its operational stage, while also providing a high degree of flexibility in its design and operation. This necessitates the careful selection of crucial decision variables in order to identify the ideal condition for high performance in order to eliminate impurities (Khajuria, 2011) . The flexibility of the PSA process is the use of operating pressure to effectively control the adsorption and subsequent preferential desorption processes.

Factors such as pore size, surface area, and adsorption capacity determine the system's selectivity, efficiency, and capacity for gas separation. Temperature and pressure control are crucial during the regeneration phase of the PSA cycle (Hao et al., 2018) as it influences the adsorption and desorption processes within the PSA system. By adjusting these parameters, PSA systems can tailor the separation process to target specific gas contaminants or impurities present in the feed gas mixture (Maniarasu et al., 2023). Maintaining optimal conditions throughout the adsorption and desorption phases, mixture can maximize the yield of purified gas while minimizing energy consumption and operating costs. Controlling temperature and pressure conditions (Raganati et al., 2021), the system can ensure effective regeneration of the adsorbent and restore its adsorption capacity, while minimizing energy consumption and maximizing the adsorbent's lifespan.

1.4 Approach

Atomistic molecular simulations, such as molecular dynamics (MD) or Monte Carlo (MC) simulations, model the behaviour of individual molecules at the atomic or molecular level. These simulations provide detailed insights into adsorption processes, including adsorbate-adsorbent interactions, surface morphology, and diffusion kinetics. Understanding the microscopic mechanisms of adsorption, predicting adsorption capacities, investigating the effect of surface modifications, and exploring adsorbate diffusion dynamics.

Classical adsorption isotherms, such as Langmuir, Freundlich, and BET (Brunauer-Emmett-Teller) models (Saadi et al., 2015), describe the equilibrium relationship between gas or liquid adsorbate concentrations and the surface coverage of adsorbent materials at the macroscopic level. Characterizing adsorption behaviour, estimating adsorption capacities, determining surface areas and pore volumes of adsorbents, and optimizing process conditions for adsorption-based separation or purification systems (Gautam et al., 2023).

Macro-scale batch equilibrium modelling involves solving mass balance equations to predict the distribution of adsorbate species between the liquid or gas phase and the adsorbent material under batch equilibrium conditions (Choi et al., 2001, Davarpanah et al., 2020). Designing and optimizing adsorption processes, conditions adsorption columns or packed beds, evaluating adsorbent performance under dynamic conditions, and estimating process parameters like breakthrough curves and loading capacities.

While each technique operates at different scales and provides unique insights into adsorption phenomena, they can be complementary in understanding and modelling adsorption processes comprehensively. Atomistic molecular simulations offer detailed molecular-level insights, classical adsorption isotherms provide semi-empirical descriptions of macroscopic behaviour, and macro-scale equilibrium modelling enables the prediction of system-level performance under practical operating conditions (Sautetj et al.). Integrating these approaches can facilitate a more comprehensive understanding of adsorption phenomena and aid in the design and optimization of adsorption-based separation processes.

1.5 Structure of the thesis

This dissertation is divided into five chapters, which are briefly summarized below.

Chapter 1: The first chapter introduces and contextualizes the whole investigation, emphasizing the purpose for the study and the intended conclusion.

Chapter 2: The second chapter provides a review of the literature, focusing on the background information on the pressure swing adsorption for separation of carbon dioxide using montmorillonite clay. Furthermore, the discussions about various types of upgrading processes, the design of experiment (DOE) knowledge, which is a tool for process optimization is clearly displayed.

Chapter 3: The third chapter describes the research approach used in this research work and the corresponding simulations conducted to achieve required objectives on the network models gives an experimental methodology with some difficulties encountered. In addition, the processes for the characterization of adsorbents are described in depth. Finally, it explains the process optimization, analytical and data simulation approaches.

Chapter 4: The findings and discussions are presented in this chapter, including comparative analysis approach. Finally, the results of RSM optimization are provided.

Chapter 5: The conclusion and recommendations are presented in this chapter. This chapter summarizes the major results of the study and draws recommendations for future works.

CHAPTER 2- LITERATURE REVIEW

2.1. Introduction

The field of bioenergy is currently experiencing rapid advancements in both technology and economics. Biogas has received significant attention from both academic and industrial sectors (Das et al., 2022). Consequently, the biogas purification market is facing significant challenges in terms of technology, energy consumption, and investment costs. Selecting the appropriate technology for biogas purification is dependent on site-specific factors, including local biomethane requirements. Thus, achieving sustainable development for biogas plants requires finding a balance between technology selection and required standards, such as selection of feedstock that is renewable and locally available. Optimizing the biogas production process to maximize energy output will require continuous evaluation of plant operations to improve efficiency and reduce costs. This chapter provides an overview of the methods that have been conducted with an aim of producing bioenergy.

Molecular simulation techniques, such as Monte Carlo simulations and molecular dynamics simulations, can provide insights into the underlying mechanisms of the separation process and aid in the design and optimization of PSA systems (Tao et al., 2022). Both methods aid to generate adsorption isotherms, which describe the relationship between the amount of adsorbate (gas) adsorbed onto the adsorbent and how gas molecules interact with porous solid adsorbent at atomic level. They can also give insights into how different factors, surface chemistry, temperature and pore size, can affect the adsorption process.

2.2. Montmorillonite

The primary component of the clay mineral montmorillonite, which is locally accessible in South Africa (a commercially exploited deposit is located close to Heidelberg in the Western Cape province), (Lasich, 2020) Montmorillonite possesses a large surface area per unit mass due to its layered structure, the characteristic provides ample active sites for gas molecules to adsorb onto the surface, facilitating gas separation (Li et al., 2011). By tuning its surface chemistry, montmorillonite can preferentially adsorb certain gas components while allowing others to pass through, enabling efficient gas separation. Montmorillonite exhibits significant swelling when hydrated, leading to an increase in interlayer spacing (Du et al., 2020). This property enhances its

gas adsorption capacity and allows for the intercalation of gas molecules between its layers, contributing to gas separation efficiency.

The regenerability allows for the repeated use of montmorillonite adsorbents, reducing operational costs and environmental impact. Its cost-effectiveness makes it an attractive option for various gas separation applications, particularly in industries where cost considerations are dominant. Montmorillonite is chemically stable under a wide range of conditions, including elevated temperatures and varying gas compositions. Its stability ensures the reliability and longevity of montmorillonite-based adsorbents as it can be regenerated by desorbing adsorbed gas molecules through temperature or pressure swing processes.

2.3. Biogas

Biogas is a renewable energy source that can be used for various energy applications. It can be utilized in combined heat and power (CHP) systems, where it is used to generate both power and heat simultaneously, space heating and cooking. Industrial processes can also use it for heat and steam production and replacing fossil fuels. Additionally, biogas can power vehicles once it undergoes a purification process to eliminate contaminants (biogas cleaning and upgrading). Nonetheless, the removal of CO₂ from methane is a crucial stage in biogas upgrading processes and is currently a major obstacle to the widespread use of biogas. Methane is the main component of biogas, which accounts for its substantial energy potential. Once it has undergone suitable processing, it can be converted into bio-methane and used as a fuel to generate electricity, thus reducing dependence on non-renewable energy sources. The use of biogas as an energy source also helps to reduce methane emissions into the atmosphere, which is highly beneficial given that methane has a global warming potential that is 23 times greater than carbon dioxide (Abdeshahian et al., 2016). There are four primary biological and chemical stages hydrolysis, acidogenesis, acetogenesis, and methanogenesis involve complicated microbial interactions to produce biogas, which is obtained by methane fermentation in anaerobic digestion (Koniuszewska et al., 2020). Methane content varies; biogas produced from agricultural waste has the highest methane content (80%), while landfill gas has the lowest (35%). It demonstrates that, depending on the kind of substrate, methane output can range from 35% to 80%. The biogas production is a viable and sustainable choice to generate a decentralized and low carbon emission-based energy economy to reduce the current environmental load partially by using a wide range of feedstock such as industrial wastewater, agricultural waste, sewage sludge and left-over carbon-based material from biodiesel and ethanol production units.

Generating sustainable energy can be accomplished by utilizing biogas, which offers a number of ecological benefits. The calorific value of biogas equals that of half a liter of diesel oil (6 kWh/m³), making it a viable alternative to other rural energy sources such as kerosene, hard coal, wood, plant residues, or propane(Koniuszewska et al., 2020). Biogas utilization can have a positive impact on the environment by reducing the release of greenhouse gases and air pollution that are associated with burning and extraction of fossil fuels which leads to degradation of environment.

The primary utilization of biogas is for the generation of electricity and Combined Heat and Power (CHP), and its incorporation into the national power grid. Similar to all other sustainable energy sources, the adoption of biogas technology would lead to a decrease of greenhouse gas (GHG) emissions and air pollution, as non-renewable fossil fuels are expected to be consumed less. In Figure 2.1, a life-cycle analysis has been carried out to compare the GHG emissions linked with different electricity production options, such as biogas, fossil fuels, and other forms of renewable energy sources. The negative emissions associated with biogas-CHP are due to replacing oil fuel with biogas(Mondal et al., 2018) .

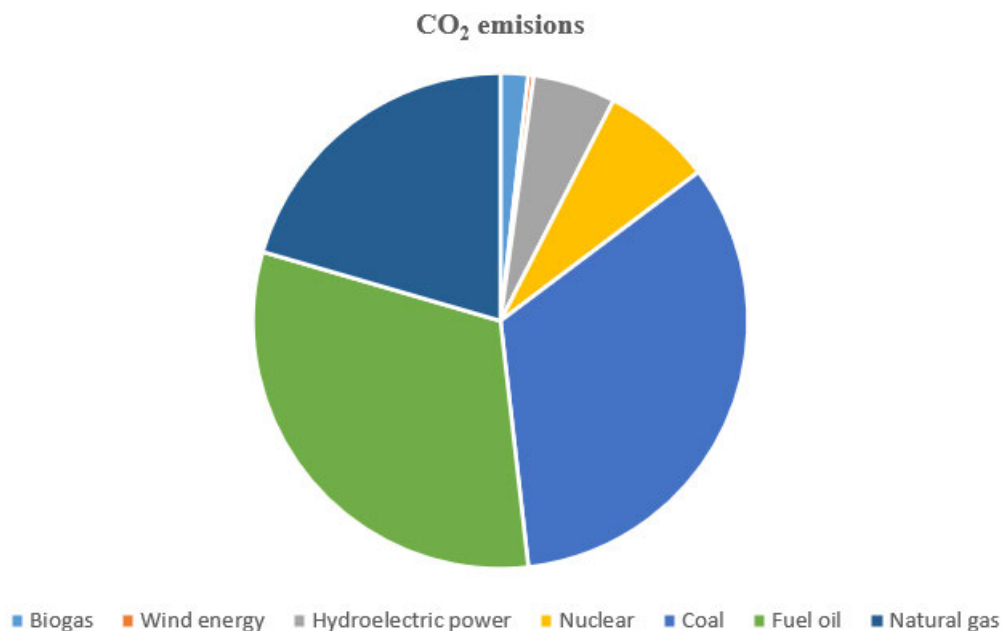


Figure 2-1 Analysis of diverse carbon dioxide discharges linked to various alternatives of power generation(Mondal et al., 2018).

2.3.1. Biogas Plants

A biogas plant is a common name for an anaerobic digester that processes farm waste or energy crops. These air-tight tanks with various configurations can generate biogas, using energy crops such as maize silage or biodegradable waste like sewage sludge and food waste. The process involves microorganisms transforming biomass waste into biogas, consisting mainly of methane and carbon dioxide, as well as digestate. Co-digesting wastewater with other residuals from dairy, sugar, or brewery industries can increase biogas yields (Achinas et al., 2017). The use of anaerobic digestion technologies for biogas production helps to reduce environmental pollution, greenhouse gas emissions, fossil fuel and chemical fertilizer usage, and improve the quality of life for rural and suburban residents (Janzen et al., 2020).

The usage of biogas as a supply of electricity is not a new idea at the worldwide level. However, in recent times, the effect of low-carbon, sustainable bioenergy programs on a nation's renewable energy have gained more interests. Figure 2.2 presents biogas plants in Europe at each country. In the European Union, there may be a growing interest in bioenergy because of the need to promote renewable energy and achieve diverse goals such as (Scarlat et al., 2018):

- lowering dependence on non-renewable fossil fuels.
- curtailing emissions that make contributions to climate change.
- creating new profits streams for the agro-forestry sector; and
- enhancing effective waste disposal.

Germany was the first country to develop biogas plants for biowaste in the 1990s. China, India, the United States of America, and European nations use biogas technology extensively and more prudently.

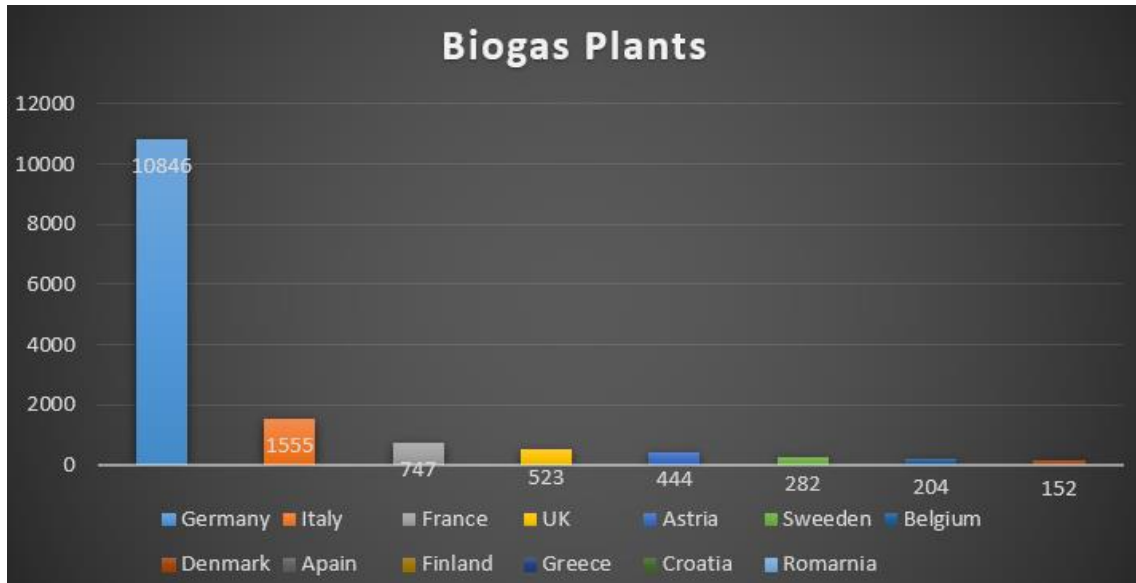


Figure 2-2 Illustration of biogas plants in Europe per country in 2015(Scarlat et al., 2018).

Despite some delays globally, especially in the next few years from 2022 to 2027, the world's biogas production is expected to continue rising with the introduction of new technologies and innovation(Mallouppas et al., 2023), demonstrating the value of biogas in the future. Various regulatory frameworks, educational programs, and technology accessibility, may provide all the person's energy needs, which reduces energy use and protects the environment(Abdul et al., 2022). The first option to meet the need for energy will be renewable energy, due to the growing environmental difficulties and problems worldwide.

2.4. Biogas Industry in South Africa

The economics of renewable energy (RE) confirm its growing significance in any future energy mix. A cost-effective way to guarantee grid and system resilience is to diversify a portfolio of resources by adding affordable RE power options(Amigun and Von Blottnitz, 2009, Mutungwazi et al., 2018). In the early days of 1957, the primary digester was installed for biogas technology in South Africa and the set up was on a pig farm located in the southern region of Johannesburg. John Fry initiated this procedure through utilising pig manure in primary 170-liter drums as digesters to fuel his six horsepower Lister engine.

Since 1962, biogas systems have not been widely implemented in South Africa, despite being recognized as a significant potential source of renewable energy in the nation(Dahunsi et al., 2020). The potential for biogas to replace fossil fuel-based energy sources and lessen reliance on

them is there due to its abundance and variety of sources. This is because of the need to move away from fossil fuels and toward sustainable energy alternatives, as well as national and international goals for renewable energy. A set of components that collaborate to generate biogas for a consumer is known as an anaerobic digestion process system(Gogela et al., 2017). The lack of significant focus given to the technology to various obstacles such as financial inadequacy and insufficient efforts to promote it. The advantages of biogas technology and the difficulties associated with its distribution, as outlined in literature, are discussed in sections 2.4 and 2.5.

2.4.1. Access to clean Renewable Energy

The biogas generated has the potential to function as a power source through the utilization of gas turbines or as gas itself. The electricity produced has the possibility of being integrated into the national power grid provided that there are adequate policies and laws in place. Attractive incentives and refunds make small-scale biogas facilities a desirable choice for farms seeking to minimize their carbon emissions and reduce electricity expenses(Gogela et al., 2017). The utilization of biogas has significant potential in addressing South Africa's energy needs. This can be accomplished through the implementation of basic biogas systems in rural regions, which can produce sufficient energy for cooking and heating. Additionally, these systems can be expanded to include community-based or commercial biogas production initiatives(Msibi and Kornelius, 2017). By establishing such systems, indoor air pollution can be reduced, illumination can be enhanced, and local employment opportunities can be created. According to Basson L. (2017), replacing fuel wood with biogas as an energy source can result in savings of R1 808 per household per year, which is equivalent to 8.6% of the household income. This equates to potential annual national cost savings of up to R4-5 billion. The potential for improving human well-being is therefore significant.

2.4.1.1. Effective Waste Management

Efficient waste management is of utmost importance for safeguarding the environment and human well-being. As per the findings of the biogas sector in South Africa is primarily devoted to waste management by diverting solid and hazardous waste away from landfills(Milanzi, 2022). However, biogas production also presents a promising source of renewable energy, particularly in rural regions where waste feedstock is abundant. Therefore, it is a suitable option for such areas, as highlighted and underscored the potential of biomass as a renewable energy resource, which encompasses several types of biomasses that can be viably transformed into

bioenergy(Rafiee et al., 2021, Yuan et al., 2022). The potential of biomass as an eco-friendly power source surpasses the yearly consumption of primary energy worldwide. Additional research has revealed that there is a possibility of deploying additional anaerobic digesters throughout the country, which can lead to cost savings by redirecting waste from landfills or employing it as a source of heat or power.

2.4.1.2. Challenges of South African Biogas Digester Industries

The challenges in South Africa are not related to the advancement of biogas digesters, but rather, there is a requirement for translational research to facilitate local production and efficient, secure, and economical implementation, especially with regards to the specific conditions in South Africa. It has been shown that the biogas digester design criteria to be considered in the selection of a suitable digester design are strength, airtightness, availability of construction materials in the locality, cost of construction, ease of operation, ease and cost of maintenance, efficiency, feasibility of insulation and reliability (Mutungwazi et al., 2018) .

a) Financial Requirements

Recent reports have highlighted that the South African biogas industry faces significant financial requirements, which is the biggest challenge to its development (Awe et al., 2017) adds that the high initial investment costs are a practical issue in biogas project development. According to, the financial viability of biogas projects in South Africa is site-specific and relies on certain conditions. The failure of projects in the country is often due to an unfavorable cost-benefit ratio, especially when electricity generation cannot be utilized as intended.

The Bronkhorstspuit initiative, for instance, took approximately seven years to initiate the project and commence the construction phase(Kaur et al., 2017). Furthermore, long-term agreements for waste management facilities present a challenge since most waste-to-energy plants necessitate a 15-20-year payback period. In order to attract investors, it may be necessary to establish comparable agreements for feedstock. However, this has been a challenge for South African organizations that focus on managing municipal solid waste, as municipalities usually have procurement contracts that are limited to three to five years.

2.5. Biogas Production

The production of biogas using anaerobic digestion is a natural biological process. The decomposition of organic materials to create biogas occurs through anaerobic digestion, which happens in oxygen deficiency environment and at certain temperatures (Bahrun et al., 2022). This process is facilitated by the interaction between various microorganisms that thrive under specific conditions. The process of anaerobic digestion, which results in biogas, can be classified into three main phases. These three stages include hydrolysis, acidogenesis, and methanogenesis. The efficiency of the anaerobic digestion process solely depends on the equal progression rate of each stage.

The subsequent stages won't proceed if any of the stages are hindered since their substrate availability will be limited, which will lower the amount of methane produced (Kapoor et al., 2017). If the third phase is shortened, the acids generated in the second phase will amass swiftly, impeding the ensuing stage.

The progression of anaerobic digestion is backed by diverse categories of specialized microorganisms that supplement each other in a consecutive fashion, with the byproducts of one microbial category acting as inputs for the following category. Consequently, the microbial categories are interlinked in a chain-like pattern, and the most vulnerable categories are the acetogenic and methanogenic categories. Microorganisms decompose organic substances (biomass) in the absence of oxygen, giving rise to methane, carbon dioxide, and water as the major byproducts. The three fundamental phases of anaerobic digestion are depicted in Figure 2.3.

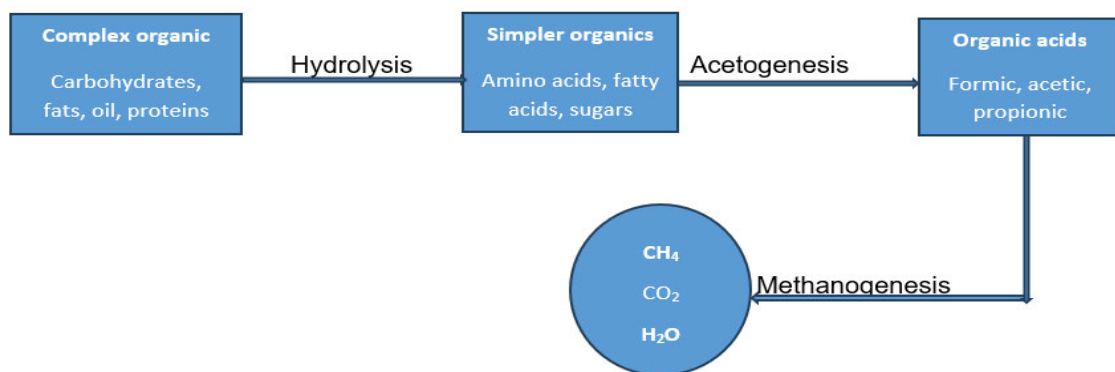


Figure 2-3 Biogas production via anaerobic digestion (Srivastava et al., 2020).

During the initial phase, which is also known as hydrolysis or liquefaction, the non-soluble and intricate organic matter, such as cellulose, is transformed into soluble compounds such as sugars, amino acids, and fatty acids by means of fermentative bacteria.

During the second phase, the outputs of the initial stage undergo a transformation process facilitated by acetogenic microorganisms, resulting in the formation of simple organic acids, hydrogen, and carbon dioxide. The process of acetogenesis is demonstrated reaction (1).



Last stage, methane is generated by methanogens, which are bacteria, using either of two methods - either by breaking down acetic acid molecules into methane and carbon dioxide or by reducing carbon dioxide with hydrogen. The former is the more prominent reaction, as the reduction of CO_2 relies on concentrated H_2 in the digesters. The methanogenesis reaction can take on various forms (equation 2.1 to 2.4):



The resulting renewable fuel has the potential to serve as a substitute energy source. Once the process of refinement eliminates CO_2 and other contaminants, the methane concentration rises, thereby allowing the resulting biomethane to act as an alternate option to conventional natural gas. After undergoing the required processing, biogas can be added to the natural gas pipeline or used as automobile fuel and also feeding into the grid, or when the project is not large enough in scale.

2.6. Biogas Upgrading

Certain pollutants are produced as reactions' byproducts when biogas is created. The utilization of biogas as a fuel source may be seriously harmed by certain contaminants present in it (Meegoda et al., 2018). Activated carbon (AC) is considered as a low cost and accessible adsorbent which consists of high surface capacities which enhance the adsorptive ability. The related study of activated carbon was conducted in separation of CO_2/N_2 operated under specific conditions of

ambient temperature and pressure swing the outcome reveals that adsorption capacity can be improved through chemical modification with metal alkalis. The PSA method is a significant advancement in gas separation that needs more research for a range of uses, most notably the upgrading of biogas.

2.6.1. Biogas Upgrading Technologies

Upgrading of biogas quality is achieved by eliminating CO₂ and other harmful impurities like H₂S which can cause harmful emissions and lead to corrosion. The energy content of biogas is directly proportional to its CH₄ content, and removing CO₂ enables a higher CH₄ content and calorific value to be achieved. The technologies used to remove CO₂ mainly involve absorption, either physical or chemical (Cozma et al., 2015), such as water scrubbing or amine scrubbing, adsorption, such as pressure swing adsorption and membranes. In addition to conventional biogas upgrading technologies, emerging alternatives such as cryogenic, *in situ* methane enrichment and hybrid are still under research and development and could eventually replace conventional biogas upgrading (Ismail et al., 2015). The purification and upgrading methods used are mainly distinguished based on their consistency, methane purity at the outlet, and methane loss during the operation process. Pressure swing adsorption and membrane technology offer promising research potential. The technology's level of maturity and vast applicability is related to lower energy consumption and costs included in the process. Lower energy consumption leads to higher net energy savings, making it more suitable for commercial and industrial purposes. The following sections describe different biogas cleaning and upgrading technologies.

2.6.1.1. Water Scrubbing

Water scrubbing is often more cost-effective than other purification methods, especially for small to medium-scale biogas plants offering high efficiency, ease of operation, and environmental compatibility. Water scrubbing efficiently removes impurities such as hydrogen sulfide (H₂S) and ammonia (NH₃) from biogas streams. It is suitable for a wide range of feedstocks and can handle fluctuations in biogas production (Ahmed et al., 2021). They can be adapted to different biogas compositions and their impurity levels. The process operations can run continuously with trivial supervision. Water scrubbing can also recover valuable byproducts such as sulfur, which can be further processed or reused in other applications, which adds value to the purification process and reduction waste.

Water scrubbing is a safe purification method, as it does not involve the use of hazardous chemicals. It eliminates the risk of chemical spills or exposure to toxic substances, making it suitable for use in various environments. It is environmentally friendly, as it does not produce harmful emissions or generate chemical waste. The process uses water as the scrubbing medium, which can be recycled or treated before disposal which contributes in minimizing operational cost of the plant. These systems can be scaled up or down to meet the needs of different biogas production facilities, (Läntelä et al., 2012) observed a decrease in CO₂ removal efficiency from 88.9 to 87.3% at 25 bar as the temperature increased from 10–15 to 20–25 °C (Xiao et al., 2014) observed that the CO₂ removal efficiency decreased from 85.3 to 52.2% as the temperature increased from 7 to 40 °C. Hence, temperature control in water scrubbing column for efficient biogas upgradation should be given great attention, especially when the plant is operated in summers. A cooling system should be used in such cases. The method is illustrated in Figure 2.4.

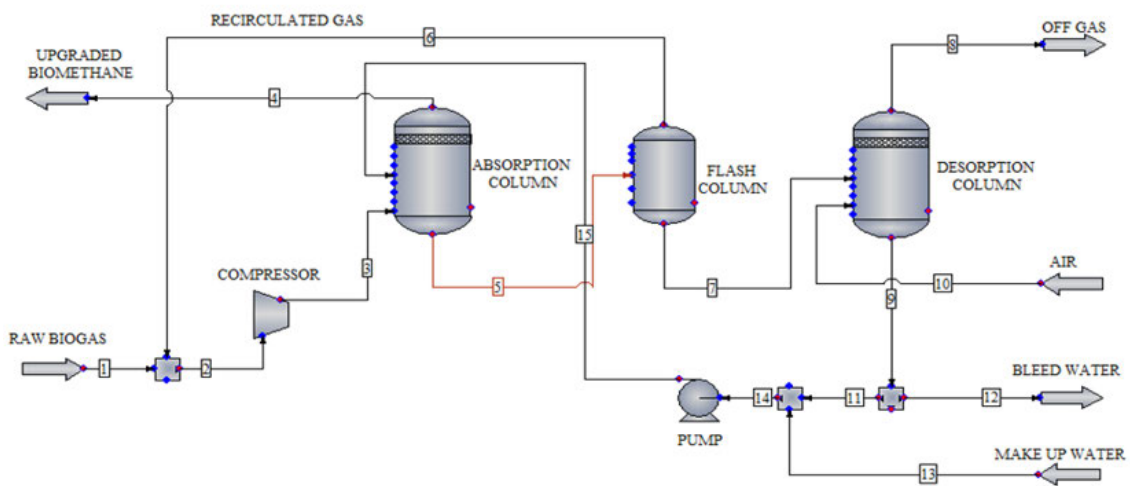


Figure 2-4 Water Scrubbing Technology (Brunetti et al., 2010)

This method relies on the difference in solubility between CO₂ and CH₄ in water. CO₂ is significantly more soluble in water at high pressures and low temperatures than CH₄. As a result, raw biogas is fed into a tower and blended with water streaming in the opposite direction, which is sprinkled from the top at a low temperature. Afterward, the CO₂-rich water is directed to another tower for the restoration process, which can be executed at high temperatures or low pressure (where the solubility of CO₂ in water decreases again). The purified CH₄ stream must be dehydrated after leaving the purifier. In this kind of technology, H₂S might also be removed together with CO₂.

2.6.2. Physical /Chemical Scrubbing

The physical scrubbing techniques are comparable to water scrubbing in terms of the fundamental principle of distinguishing between solubility of CO₂ and CH₄. Nevertheless, instead of water, organic solvents such as polyethylene glycol are employed to dissolve CO₂. They offer flexibility in design and implementation, allowing for integration into existing infrastructure. These methods can simultaneously remove multiple impurities from biogas streams, offering comprehensive treatment and ensuring compliance with quality standards for various end uses, such as power generation, heating, or vehicle fuel. Chemical/physical scrubbing systems allow for precise control over purification parameters (Cavaignac et al., 2021, Upadhyay et al., 2022), such as temperature, pressure, and chemical dosing rates, optimizing performance and ensuring efficient operation. Energy requirement during the process is mainly for gas compression, water pumping and regeneration. Investment costs of water scrubbing systems depend upon the scale of the plant (Bauer et al. 2013). As the plant capacity increases, the cost decreases. W.

The solubility of CO₂ in these solvents is greater than that in water. Consequently, the efficiency of a chemical scrubbing system can surpass that of a water scrubbing system with equivalent capacity. Dehydrated and compacted biomethane is inserted at the base of the absorption tower, while the cooled natural solvent flows from the top to create a counter-current flow of gas and liquid. Afterward, the natural solvent is directed to the flash tank (Mohanakrishnan et al., 2016), where methane with a small amount of impurities is released under low pressure and recycled. The solvent then enters the desorption column to be regenerated. Because natural solvents are resistant to corrosion (Ahmed et al., 2021), the scrubber's pipeline doesn't have to be made of stainless steel, which can save on investment capital and make installation and maintenance easier. Additionally, depending on the system's design, it can be operated at low temperatures without the need for extra heat due to the natural solvent's low freezing point. The

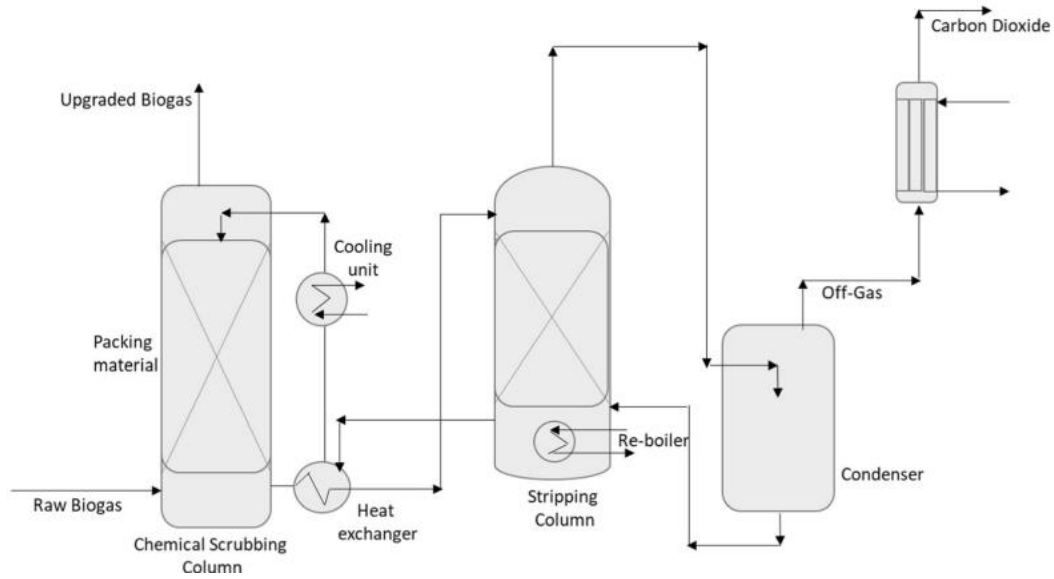


Figure 2-5 Biogas upgrading by chemical absorption amine scrubbing(Cavaignac et al., 2021).

Scrubbing technology that employs chemicals like mono-ethanol amine and di-methyl ethanol amine is utilized to dissolve CO₂. Nonetheless, a chemical reaction transpires between the CO₂ and the solvent, resulting in the creation of a fresh solution. Amines have a great attraction for CO₂, which makes it feasible to attain high levels of purity and retrieval using such solvents. The column where the chemical absorption process is transpiring can be regenerated with the help of vacuum (low pressure) or heat (high temperature)(Ghatak and Mahanta, 2016). The pre-pressurized unprocessed biogas is introduced from the lower part of the absorber as the amine-derived solution (AmH) is introduced from the upper part. This creates contact with a counterflow, where the CO₂ is absorbed into the solvent used. Once the absorption process is completed, biomethane is obtained from the upper section of the columns. Simultaneously, the fluid is conveyed to the upper section of the stripper column through a heat exchanger, where it encounters a packing substance that encounters steam to discharge CO₂.

2.6.3. Membrane Technology

In most cases, a membrane refers to a solid layer, although it may occasionally be a thin fluid layer. The process of separation relies on a chemical or physical bond between the membrane material and a specific gas. The movement across the membrane is propelled by a gradient in chemical potential. The membrane's composition and design dictate the rate of flow. Membrane separation methods are categorized based on pore size and the driving force. Examples of these

classifications include ion-exchange, reverse osmosis, nanofiltration, ultrafiltration, and microfiltration (Bernardo and Clarizia, 2013, Drioli et al., 2011). There are numerous aspects to contemplate for the effective utilization of membrane separation. In order for the membrane to function, it is imperative that a pressure differential is upheld across it. This enables gases with high permeability to pass through while gases with low permeability are retained. As a result, the feed must be obtainable at an appropriate pressure, typically high. While it may not be feasible to achieve high purity recovery in all cases, applications that necessitate moderate purity can be examined. Additionally, selectivity plays a crucial role in the successful separation process. It is essential that the feed does not contain any hazardous materials that may cause damage to the membrane (Zhou et al., 2017).

Currently, membrane processes are widely used to upgrade biogas due to their simple operation and lack of chemicals or heat. This technology operates by permeating gas or liquid through the membrane filters and is dependent on the concentration gradient of the permeator. Choosing the right type of membrane is essential to the technology's efficacy. It is lightweight, compact, and requires minimal labor for plant maintenance. Unlike other upgrading technologies that depend on the concentration of volatile organic compounds (VOCs) in the biogas, the membrane process is not affected by the concentration of VOCs. Figure 2.5 shows a 2-stage membrane process biogas upgrading process.

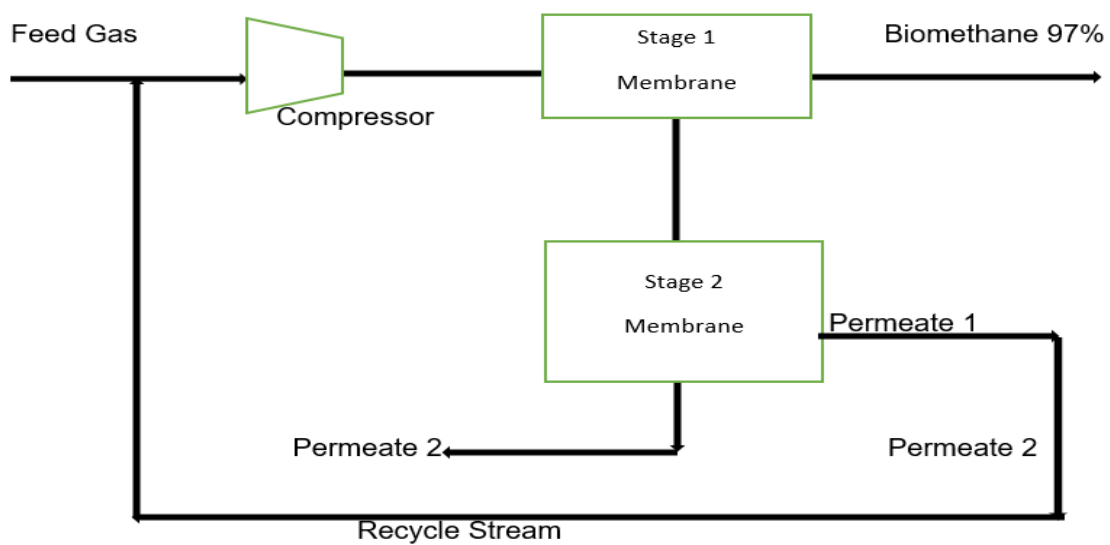


Figure 2-6 Two Stage Membrane Process Biogas Upgrading process (Zhou et al., 2017)

A key benefit of membrane separations is their simple installation and usage. Additional benefits include convenient scalability thanks to a modular layout, absence of any phase alteration, no requirement for chemical supplements, potential for recycling, and uninterrupted steady-state operation (Gkotsis et al., 2023). Despite numerous benefits, membrane technology also presents certain drawbacks, including the high cost of membranes, the degradation of membrane filters over time, and membrane damage caused by vibrations from colloidal solids (Hashemifard et al., 2011). However, there exist numerous obstacles when it comes to utilizing membranes.

These barriers include fouling and cake formation, which can lead to a decrease in effectiveness over time. While concentration polarization may not be as prominent in gas separation, it still poses a challenge. To address fouling, cleaning and purging with non-adsorbing gases can be employed, as well as prefeed filters to mitigate the issue to a certain extent. Additionally, high pressure can trigger compaction, causing a reduction in pore size for polymeric membranes. Sustaining the pressure is the sole task that requires significant energy input. As the majority of flue gases comprise a negligible proportion of CO₂, the resident time prolonged. Consequently, the operation must continue for an extended period, leading to increased expenses. To be applicable for industrial-scale separation, the membrane must exhibit a high degree of selectivity towards CO₂. In addition, the membranes are designed in such a way that they are incapable of withstanding temperatures exceeding 100°C (Ji and Zhao, 2017).

2.6.4. Cryogenic Separation

Cryogenic separation can achieve very high purity levels in the purified biogas, particularly in terms of methane content. Their processes are highly efficient in removing impurities such as carbon dioxide (CO₂), hydrogen sulfide (H₂S), water vapor (H₂O), and other contaminants, resulting in a biogas product with superior quality. Cryogenic separation allows for selective separation of gases based on their boiling points even at low temperatures (Yousef et al., 2018), leading to effective purification with minimal energy consumption. Methane, which has a lower boiling point compared to other impurities, can be selectively captured and recovered, while other impurities such as CO₂ or H₂S can be recovered for further processing or reused in other applications as valuable byproducts.

The process provides a clean and environmentally friendly purification method, as it does not involve the use of chemicals or generate harmful emissions and reduction of waste (Baena-Moreno et al., 2019). They can operate continuously with minimal maintenance requirements, providing

consistent performance over extended periods. It relies on physical principles of gas separation, making it a sustainable option for biogas upgrade. Cryogenic separation systems are known for their reliability and long-term stability (Karne et al., 2023). They are suitable for applications requiring premium-grade biogas for use in power generation, heating, or transportation. They offer flexibility in design and implementation, making them suitable for both small-scale and large-scale biogas production facilities.

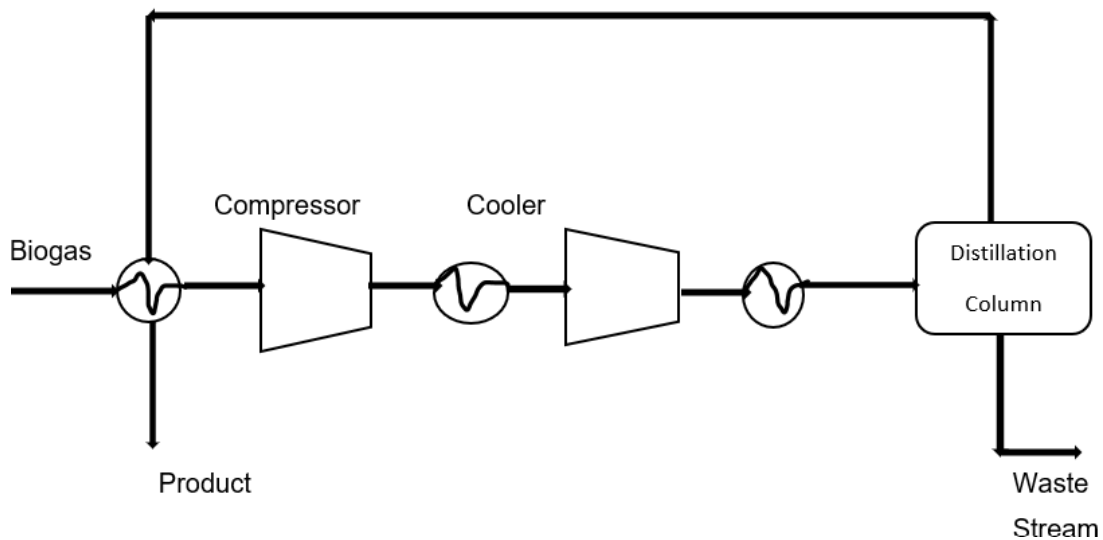


Figure 2-7 Biogas upgrading procedure by cryogenic separation (Baena-Moreno et al., 2019)

This process entails segregating gas blends through fractional condensation and low-temperature distillations. The raw biogas is pressurized to roughly 8 000 kPa and subsequently dried to prevent freezing during cooling as shown in Figure 2.6. The biogas is then cooled to -45°C , and the separator eliminates condensed CO_2 . The CO_2 is then further treated to retrieve dissolved methane (Naquash et al., 2022), which is recycled back to the gas inlet. This process yields methane with a purity of 97%, which is attained in the form of liquid that can be easily transported. Despite its benefits, the method has some drawbacks, including high capital costs and complex equipment requirements (Yusuf and Almomani, 2023).

2.7. Pressure Swing Adsorption (PSA)

The technology used for upgrading biogas, called Pressure Swing Adsorption (PSA), relies on separating CO₂ and other non-calorific gases such as N₂ and H₂S. Understanding the molecular composition allows for assessing the economic viability and potential applications for biogas production that is used to evaluate the necessary treatments (Bahrun et al., 2022) and upgrading technologies to meet desired quality specifications. The PSA unit operates in a predetermined cycle consisting of several steps. The first step is pressurization, where the adsorbent-filled column is pressurized to the desired level for the production phase. During the production phase, which takes place at high pressure, CO₂ is adsorbed while CH₄ is produced. Just before the CO₂ ruptures, a blowdown phase begins to prepare the vessel for the low-pressure regeneration phase. During regeneration, or purge, CO₂ is released from the adsorbent by passing a product gas or an inert gas counter-currently through the column. The column is then ready for a new cycle.

Adsorption refers to the phenomenon where a gas or liquid molecule attaches itself to the surface of a specific solid material, causing the molecules to be held on the surface of the solid, which is known as the adsorbent. The molecules that are held on the surface of the adsorbent are referred to as the adsorbate. The process is spontaneous and releases energy, and the amount of adsorbate retained in the adsorbent is dependent on the material selected and environmental elements (Abd et al., 2021).

The adsorption techniques can depend on two mechanisms: kinetics and equilibrium. Separations that rely on kinetics are achieved by utilizing the difference in diffusion rates of different molecules into the adsorbent pores. This type of separation is possible only in adsorbents that depend on kinetics, for instance, carbon molecular sieves (CMS). Conversely, separations that rely on equilibrium depend on the different abilities of the adsorbent to hold various types of molecules.

At a specific temperature and pressure, the interaction between an adsorbent and a molecule leads to an equilibrium state between the adsorbed phase and the concentration of the adsorbate in the fluid phase. This occurrence is commonly depicted by adsorption equilibrium isotherms (S., 2010), which establish a correlation between the amount of adsorbate in kilogram of adsorbent with pressure and concentration.

Due to the low capital investment, the PSA process is of great interest. PSA can be efficiently used for large-scale production of biomethane compared to membrane-based technologies (S., 2010). Additionally, the oxygen content in PSA technology can be reduced to 0.2-0.5% by volume, whereas in other products the oxygen is not removed by processes (S., 2010) such as physical scrubbers. Oxygen can cause irreversible damage to amines in the amine scrubbing process. PSA technology poses the opportunity of removing nitrogen. Most techniques are also described, depending on the sorbent used. The standard configuration does not remove nitrogen. In addition to the above reasons, power consumption at high speed is low. The PSA regeneration process is one of the most commonly used commercial processes.

2.7.1. Principles of Pressure Swing Adsorption

PSA unit has been a mature technology and there is active research and development on improving processes, selecting new adsorbents, and designing new adsorbents. The fundamental concept behind the PSA operational process is uncomplicated. At first, a mixture of gas is guided towards a bed filled with particles that adsorb - this is referred to as the adsorption phase. In the PSA column, gases are selectively separated, producing a stream with a high concentration of light product, which is the compound that is least adsorbed. The adsorber has a zone with a concentration gradient ranging from zero to equilibrium, termed the mass transfer zone (MTZ), and this is where the adsorption process occurs at a given moment. To avoid the adsorbent from becoming saturated and contaminating the resulting product, the adsorption phase halts before the MTZ front traverses the entire column. Afterwards, the column is depressurized to facilitate the regeneration of the bed by desorbing impurities - this is the depressurization phase. Regeneration is assisted by a purge that contains a small amount of purified light product or an inert gas - this is the purge phase. Finally, the column is partially pressurized, typically by introducing feed gas, to initiate the cycle once again - this is the pressurization phase.

The Skarstrom cycle, a basic four-step process applicable to two beds, can be enhanced through the use of pressure equalization steps. To integrate these steps into the cycle, an additional connection between the top of one column and the bottom of another must be established. Once high-pressure adsorption has occurred in one bed and low-pressure purging in the other, the pressures in both can be equalized. This step is an alternative that can improve separation efficiency and energy conservation in a simple PSA cycle. Another option is vacuum pressure

swing adsorption (VPSA)(Abd et al., 2021), which replaces low-pressure purging with vacuum desorption. This method saves products that would otherwise be lost in the off-gas stream during purging. Although VPSA systems consume more energy due to the need for vacuum pumps and higher adsorber regeneration energy, they are a viable option for reducing product losses(S., 2010) . The PSA method boasts several benefits, including minimal energy consumption, chemical-free operation, and economical maintenance. Additionally, it is a reliable and well-established technology with numerous operational units in the industrial sector. However, there are also a few drawbacks to consider, such as the necessary supplementary unit to eliminate H₂S (and often water) prior to the PSA unit, a rigorous process control requirement for cycle regulation, and costly maintenance due to the frequent switching of many valves within the system.

2.8. Literature Survey on Research Performed to upgrade Biogas quality.

Compared the purification of biogas by clay through dry adsorption and wet carbonation procedures(S., 2010), which had not been attempted before. The scientists utilized X-ray fluorescence to characterize the natural and altered clay. Gas chromatography and digital biogas analyzers were utilized to examine the composition of the biogas. The CAVS adsorption software was used to examine the carbon dioxide removal process's breakthrough curves, kinetics isotherm, and adsorption equilibrium. It was discovered that 75°C and a clay-to-water ratio of 1:3 were the ideal slurry temperatures and ratios for CO₂ absorption during the carbonation process. The results indicated that the carbonation process resulted in a pH drop from 9.2 to 6. Additionally, the results showed that the modified clay had the maximum capacity to absorb CO₂ (5.72 mmol/g), and complete elimination of hydrogen sulfide was achieved. The CO₂ absorption capability dropped as the adsorbent mass-to-biogas volume ratio started dropping. However, the CO₂ removal efficiency reached a maximum of 93.8% at a ratio of 7 g/L. As a result, modified clay has the potential to be a promising option for purifying biogas.

Karne et al (2023) devised a numerical framework to effectively portray the dynamic functionality of activated carbon derived from biomass in the refining of biogas. This research signaled the start of the initial phase in creating a carbon capture system that is based on biomass, in the context of circular economy and bioenergy. The adsorbent material chosen was microporous activated carbon pellets, which were derived from pine sawdust through physical activation using CO₂. The Langmuir-Freundlich model was used to fit the single-component adsorption isotherms of CO₂ and CH₄ at different temperatures, while the Ideal Adsorbed Solution Theory (IAST) was utilized to consider multicomponent adsorption. The separation efficiency of a biomaterial-based PSA

process for biogas refining was assessed using the model(Khajuria, 2011), and the impact of important performance parameters was ascertained by a parametric analysis. According to the sensitivity study, in a setup with P/F ratios (ratios of molar fluxes of CH₄ in the purge and feed streams) ranging from 0.67 to 1 with an adsorption pressure of 300 kPa, a single stage 4-step PSA may produce methane with a purity of over 95% and a recovery rate of over 60%.

Conducted experimental analysis to enhance the quality of raw biogas by increasing its calorific value and eliminating undesirable components(Bahrn et al., 2022).The experimental findings indicate that novel techniques are capable of reducing the acidic content (H₂S) by 99% and eliminating the CO₂ content by 82%. Consequently, the methane content increased from 56.7% to 85%, while the CO₂ content diminished from 36% to 7%. Based on the results, it can be inferred that chemical purification process is the most effective method to upgrade biogas by augmenting the CH₄ concentration. Among the two methods used in the experiment, method 1 of using NaOH, activated carbon, and silcagel was found to be superior to method 2 of using KOH, wood charcoal, and silcagel. The research highly recommended more work to be performed on economic analysis to verify ways in which additional cost incurred in upgrading biogas can be recouped by selling the upgraded biogas. This research also recommended future studies on alternative biogas upgrading technologies to be explored to identify the most efficient, economical, and environmentally friendly options.

Executed the development and construction of a 1 cubic meter biogas digester for households and simulated its functionality by utilizing donkey manure as a biogas substrate(S., 2010). A mathematical model was created using MATLAB to calculate the methane output of donkey manure based on pH, COD, NH₄-N, digester temperature (TD), and total alkalinity (TA). The biogas digester design was successful in producing biogas with an average methane yield of 55% when supplied with donkey manure as a single substrate. According to this study, additional research is required to identify bacteria genera that can endure temperature changes in a biogas digester while still generating biogas. Furthermore, more investigation can be conducted on a batch biogas digester to generate additional dependable data.

(Bahrn et al., 2022)Performed an examination process of enhancing biogas through adsorption utilizing commercial carbonaceous adsorbents. The experiment was executed using CO₂/CH₄ mixtures of varying concentrations as feed gas in a fixed-bed column. The study revealed that Desotec's activated charcoal (AC) had a higher capacity to adsorb both CO₂ and CH₄ and superior kinetic performance compared to carbon molecular sieves (CMSs) made by Carbotech and

Xintao. However, the results showed that CMSs had a significantly lower CH₄ adsorption capacity than AC due to their thermodynamic/kinetic sieving properties. CMSs also exhibited greater selectivity for separating CO₂/CH₄ mixtures, with Xintao's sample performing better due to its faster kinetics and complete regenerability. The use of MATLAB for breakthrough curve modeling indicated that intraparticle diffusion was the limiting factor for CO₂ adsorption. The research concluded that CMSs are more effective in enhancing biogas due to their adsorption capacity to remove CO₂.

(S., 2010) Formulated a set of mathematical models that can facilitate in anticipating the efficiency of biogas refinement methods that involve hydrogen infusion within the system, which is still a demanding task. In this particular study, an existing model on anaerobic digestion was revised and extended to include the impact of hydrogen injection into the liquid phase of a fermenter. The objective was to model and simulate these procedures proficiently. The model encompassed hydrogenotrophic methanogen kinetics for the consumption of H₂ and an inhibitory effect on acetogenic stages. The transfer of H₂ from gas to liquid was given significant consideration. The model was effectively authenticated through a sequence of Case Studies, with the biogas composition and H₂ utilization being accurately anticipated. The overall variation from experimental measurements was less than 10%. Parameter sensitivity analysis demonstrated that the model is highly responsive to the H₂ injection rate and mass transfer coefficient. Hence, this model is an efficient instrument for forecasting process efficiency in biogas refinement situations.

(S., 2010) Conducted an optimization procedure for biogas refining to meet fuel quality standards using a plate PSA configuration. The procedure utilized unprocessed biomass adsorbent under non-isothermal and non-adiabatic conditions. A central composite design was used to examine the effects of system pressure, CO₂ concentration, and adsorption/desorption duration on the purity of CO₂ in the waste stream and bioCH₄ in the product stream (S., 2010). The response surface methodology and desirability function were employed to establish the most favorable points of the factors to maximize the purity of bioCH₄ and CO₂. The quadratic model produced was characterized by an experimental error of less than 5% and demonstrated that the factors had a significant impact on both outcomes.

On a desire scale of 0.95-1, the best parameters for bioCH₄ purity were an adsorption period of less than 5.9 minutes, a CO₂ concentration below 50%, and a system pressure between 170 and 300 kPa. On the other hand, the ideal parameters for CO₂ purity in the waste stream were CO₂

concentration above 65%, system pressure above 250 kPa, and desorption time of 6 minutes. Utilizing these ranges of parameters, the biogas refining system produced 97% pure biomethane.

The study considers various factors, including heat transfer conditions, biogas mixtures, axial mass dispersion coefficient, and cooling outside column wall. (Abd et al., 2021, Ahmed et al., 2021) Utilized PSA technology to enhance biogas quality through one-dimensional binary mixture adsorption, heat and mass transfer modelling with Aspen Adsorption™ version 10. Experimental data on zeolite NaUSY is used to validate the model, with reasonable agreement shown in the CO₂ breakthrough curve. The results indicate that reducing heat during adsorption can improve methane purity and recovery.

Natural, earthy, fine-grained clay becomes malleable when combined with a small quantity of water. Clays are composed structurally of layers of tetrahedral and octahedral sheets. Hectorite, saponite, and montmorillonite (Hashemifard et al., 2011) are the three-layered silicates that are most frequently found. Negative charge delocalization is made possible by the clay layers. Due to their high hydrophilic nature, water molecules typically occupy the space between clay layers. They can absorb certain cations and hold them in an exchangeable state, allowing other cations in a water solution to exchange for intercalated cations (Xiao et al., 2014). Most of the inorganic fillers employed in montmorillonite are materials of the porous molecular-sieve type, such as carbon molecular sieves and zeolites. In comparison to a polymeric membrane, the addition of molecular-sieve type fillers to a polymer matrix typically results in increased permeability (S., 2010), selectivity, or both.

Grand Canonical Monte Carlo Simulation (GCMC) method was first proposed by Adams in 1975. This approach can exchange the number of particles as well as energy across systems. Consequently (S., 2010), its primary application is in systems whose particle count varies in response to variations in external factors. Simulation studies has been conducted using this method (Tao et al., 2022) carried out research on three different Metal-Organic Frameworks (MOFs) to capture CO₂. The CO₂ adsorption capacity of MOFs was shown to be improved by the presence of coordinated unsaturated metal sites, as evidenced by the adsorption and separation behaviour of pure CO₂ and CO₂/N₂ from their surface area.

The aim of this study is to assess the feasibility of the newly developed montmorillonite clay used to separate undesirable sour components from biogas, specifically CO₂ and H₂S. This study also investigates the conditions of multicomponent molecular simulations of biogas blends with MMT as in a Pressure Swing Adsorption system by generating adsorption isotherm(S., 2010). The details of the procedure conducted is presented in chapter 3. There are significant economies of scale for all the technologies investigated in the past which are most focusing on improving sustainable energy sources and environmental protection by reducing CO₂ emissions. The use of natural adsorbent has been explored in the literature with different technologies with its limitations.

2.9. Previous studies

The ability of montmorillonite nano-clay to store nitrogen, carbon dioxide, and methane at high pressure was investigated. As montmorillonite is found in depleted shale reservoirs, adsorption data were gathered to investigate and evaluate its potential uses in gas storage. The thermodynamic characteristics of montmorillonite and its amine-impregnated structures were assessed using energy dispersive X-ray spectroscopies, Fourier transform infrared, thermogravimetric analysis, and thermogravimetric analysis(S., 2010). The next step was using a high-pressure magnetic suspension sorption device at 298 and 323 K isotherms up to 5 x10³ kPa, low- and high-pressure gas sorption experimental investigations were carried out. Based on single gas adsorption experiments, the selectivity of each gas on each nano-clay material were computed and provided in the text. Furthermore, the kinetics and heat of adsorption are computed and reported. The behavior of CO₂ at various montmorillonite clay specifications is shown in Figure 2-7.

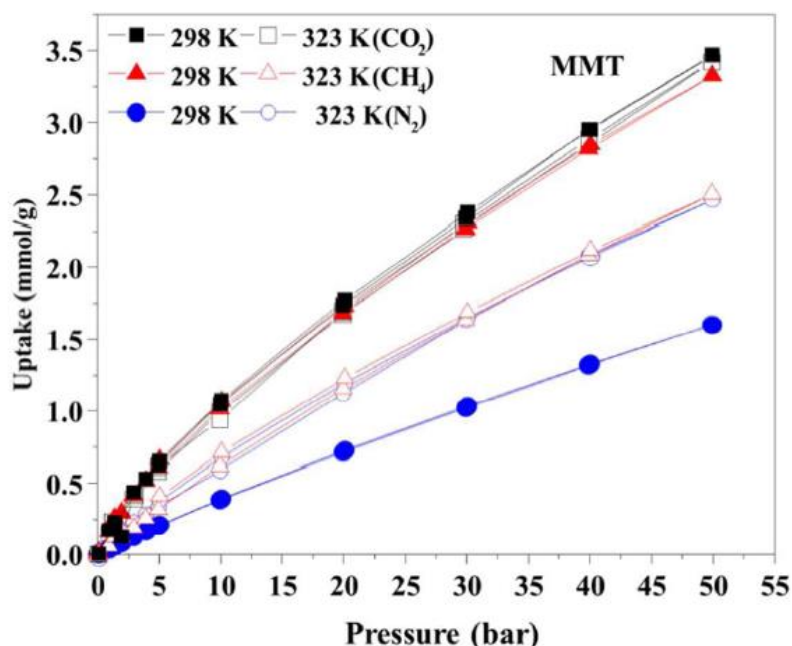


Figure 2-8: CO₂, CH₄, N₂ adsorption at low pressure from 0 to 10 Bar and 298K(Azizian and Eris, 2021).

Heller et al investigated the sorption of methane, carbon dioxide, and perhaps nitrogen on mineral samples and gas shale as well as the use of MMT. Since MMT has a limited capacity for CO₂ sorption on its own, a number of different modifications and procedures, including optimization, shale composition and surface modification, microstructure and morphology control, and control, have been proposed to increase MMT's CO₂ capture capacity and selectivity.

For CO₂ capture (S., 2010) suggested circulating a gas containing CO₂ through a bed of MMT adsorbent that has been treated with amine. However (Stevens et al 2013) also created diamine-impregnated MMT via grafting and water-assisted exfoliation, and they were able to attain 2.4 mmol g⁻¹ CO₂ adsorption capture performance at 100 °C. In their study (Heller et al 2014) employed MMT nanoclays that had not been treated or modified with amines. They observed that the performance of CO₂ capture was significantly enhanced when the nanoclays were doped with amines.

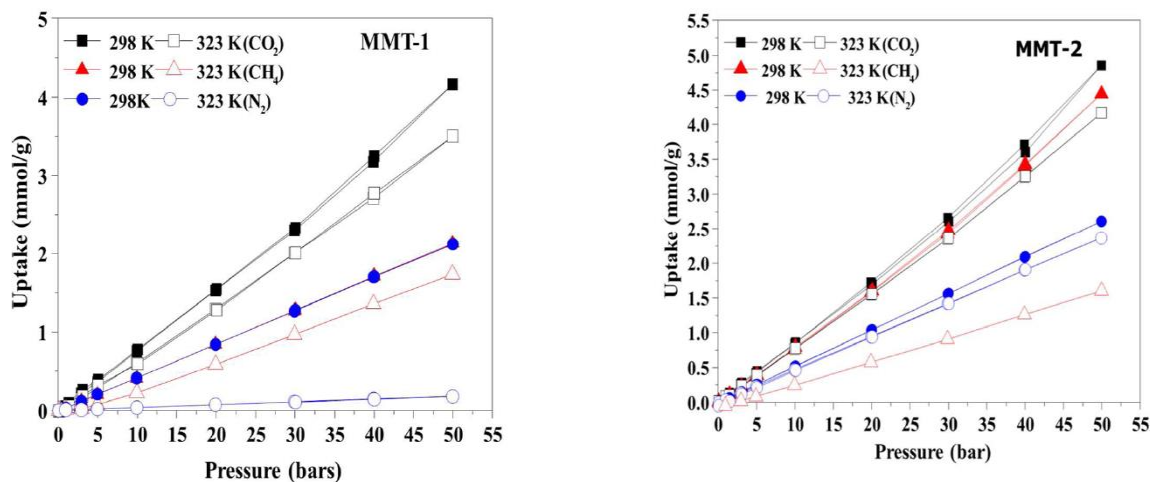


Figure 2-9: Adsorption isotherms for the components between MMT1-MMT at 50 bar and, 298 and 323 K (S., 2010)

The CO₂ adsorption by MMT at the two temperatures was nearly equal, despite the fact that the adsorption capacities of N₂ and CH₄ varied considerably. The findings indicate that N₂ intake rises with temperature. It is noteworthy that MMT collects more N₂ at higher temperatures than at lower ones, in contrast to other solid sorbents. It's interesting to note that the amount of CO₂ and CH₄ absorbed at room temperature was comparable to the amount of N₂ under comparable circumstances. The adsorption behavior of MMT is essentially incomparable to that of other solid materials at these specific pressure and temperature circumstances. CH₄ and CO₂ at 298 K behave the same, and N₂ uptake increases as temperature rises because CO₂ adsorption is almost the same at both temperatures. It was discovered that the maximum amount of CO₂ adsorbed was somewhat lower at the higher temperature of 323 K because all of the materials underwent an exothermic reaction.

The adsorption capacity reveals that MMT adsorbs almost an equivalent or even more quantity of CO₂ in the pressure ranges of 8 and 20 bar at 298 and 323 K, respectively, than amine impregnated materials. This unique behaviour can be associated with larger pore volume and surface area of the nonmodified material. The findings demonstrate that as temperature rises, basal spacing and interlamellar space are squeezed, leading to structural instability and a considerable decrease in MMT's pore volume and surface area. MMT has an acidic disposition that is highly structural dependent and affects its catalytic capabilities. In octahedrally substituted MMT, calcination moves protons into the sheet vacancies and expels them.

The modified montmorillonite containing octadecyl-amine (ODA) was found to have a higher ability to collect CO₂ than all other modified nanoclay samples and commercial adsorbents including zeolites and activated carbon. The binary selectivity of all the materials is based on the maximal uptake at various temperatures, and the selectivity of adsorbents is equally important as capture capacity. At room temperature, MMT exhibits extremely low selectivity for CO₂: CH₄:N₂, which is decreased even further to nearly zero at high temperatures (323 K). This indicates that at greater pressures and temperatures, unmodified montmorillonite absorbed almost the same quantity of various gases. Figure 2-9. Present how the temperature affects the adsorbent structure (MMT, MMT-1, MMT-2 and MMT-3) as the temperature profile changes within the process.

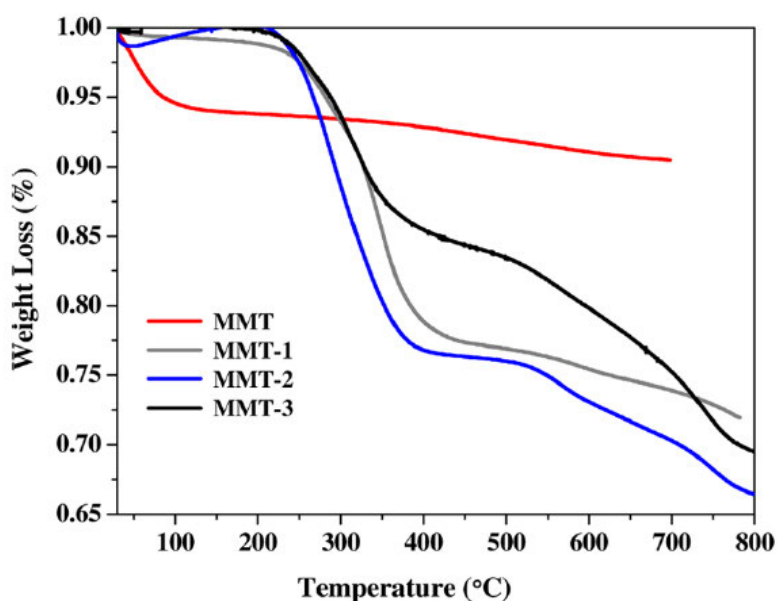


Figure 2-10: Thermal gravimetric analysis of nano modified and amino modified clay(S., 2010).

The unmodified nanoclay sample, according to analysis, was stable up to 300°C; nevertheless, there was a 5% weight loss in the materials, which was mostly caused by the water that had been stored in them. The second loss, which was linked to the extremely sluggish breakdown of nanoclays, began at about 300°C and resulted in an additional 4% loss in material weight. The thermal investigation indicates that the unmodified material has demonstrated excellent stability, as evidenced by its extremely low breakdown rate of 8% at temperatures as high as 700 °C. However, in all amine-modified materials, a three-step breakdown was seen, with the

temperatures being set at 270 °C (5%), 400 °C (15%), and 560 °C (35%). The initial 15% decomposition of changed materials can be attributed to the burning of the amine group, while the remaining 35% can be attributed to the loss of nanoclays, indicating material instability over 400 °C.

Almost identical results were reported for all nanoclay materials treated with different organic moieties, such as ethylene glycol.¹⁶ It is worth noting that all of the materials have demonstrated good thermal stability up to 270 °C. The materials were measured with a Micromeritics ASAP 2420 surface and porosity analyzer for Brunauer-Emmett-Teller (BET) and degassed. The results of BET analysis using liquid nitrogen are displayed in Table 3.2. The pure nanoclay material's BET surface area and pore volume are determined to be 253 m²/g and 0.42 cm³/g, respectively.

Table 2-1 Physical properties and BET Analysis of Nano clays materials.

Sample	Density	Pore volume	BET surface area	Pore size
MMT	0.59	0.42	253.42	6.50
MMT-1	0.44	0.09	12.29	29.50
MMT-2	0.37	0.05	8.47	24.80
MMT-3	0.34	0.11	11.82	37.00

These values are noticeable greater than those of the changed materials. Physical properties reveal that after impregnation with APTS (aminopropyltriethoxysilane), DDA (dimethyl dialkyl amine), and ODA (octadecylamine), the surface area and pore volume are significantly reduced, indicating incorporation of various amines into the porous structures of the nanoclays. Importantly, amine modification also had an impact on density. Although, the surface area and pore volumes of the materials were reduced significantly, however, it was proven that affinity of CO₂ enhanced due to the attachment of the function group on the surface and inner pores of the materials. Such effect of reduction in the physical properties but enhancement in the affinity of CO₂ in the solid sorbents such as mesoporous silica, metal organic framework, activated carbon and nanomaterials.

2.10. Biogas upgrade technology limitations

Sustainable renewable energy sources do not only assist infrastructure or communities but may also increase energy production in the Energy and Mineral Resources sector. Furthermore, they contribute to environmental conservation and the general improvement of energy sources. This also applies to the EU-27 countries, for which it is a chance to achieve the assumed objectives in the field of environmental protection, but also because it makes it possible to become independent from external energy supplies, which in turn leads to increased energy security (Pacesila et al, 2016) found that domestic renewable energy production can reduce energy dependence in any country.

The accumulation of waste due to farming has led to an increase in CH₄ and CO₂ production. If the greenhouse effect results in an increasing temperature rise on our planet, there is a risk that when organic materials are progressively decomposed in large areas will result in huge quantities of methane being released. The current technologies for biogas production are still not efficient. Although the biogas plants available today can be able to meet some energy needs, provided the energy sector's willingness to invest in the new technology for improving renewable energy sources. The biogas production like other renewable energy sources (e.g. Wind and Solar) biogas generation are also affected by the weather(Dehghani, 2020), which will lead to unstable operation on day to day basis and increase operational cost.

Although each technology has high removal efficiency for CO₂ and H₂S, providing high-purity biogas and the low operational cost, maintaining a stable operation becomes demanding as it is depended to the biogas production. This means large scale production to supply for a large biogas plants are still not possible at the current state. Therefore, the market for biogas upgrading will most likely be characterized by harder competition with the establishment of new upgrading technologies and further optimization of the mature technology to decrease operation costs.

CHAPTER 3-MATERIALS AND METHODS

3.1. Introduction

This chapter presents the methodology implemented in this study, which focuses on the effectiveness of a novel adsorber in purifying biogas. The chapter offers insight into the research design, Monte Carlo simulation, data collection, experimental procedure, data analysis, and the validation of results. The research utilizes a simulation-based approach, providing a quantitative analysis of the effectiveness of the novel adsorber. The efficiency and the simplicity of Monte Carlo simulations makes the tool more valuable for modeling complex systems, incorporating randomness and uncertainty, validating models, performing sensitivity analysis, solving integration problems, optimizing parameters(Tao et al., 2022), and leveraging parallel computing resources. They are widely used across various fields to address a wide range of challenging problems. With the new improved technology, conducting simulations using the GCMC approach aids to explore other methods with less time processing compared to other methods used in the past. This method can also benefit industries with large-scale process for better performances and plant optimization. The selected research design supports detailed investigation into the relationship between input variables and resultant biogas purity.

3.2. Montmorillonite

Montmorillonite has a unique structure characterized by thin, flat layers that can easily slide over one another as shown in Figure 3.1. This property gives it high swelling capacity and makes it useful for its excellent adsorption capabilities(CLA), especially for heavy metals and organic pollutants. Montmorillonite has several distinct physical properties and a specific chemical formula: $\text{Ca}_{0.33}\text{Al}_{1.67}\text{Mg}_{0.33}\text{Si}_4\text{O}_{10}(\text{OH})_2$. The clay minerals are heterogeneous with varying compositions and particle sizes. These materials' potential as catalysts and/or catalyst supports(Hashemifard et al., 2011), as well as their well-defined layered structures and flexible adsorption qualities, are what led to their usage in the development of clay-modified electrodes (CME).

Montmorillonite clay has principal intercalated cations being alkaline earth ions and alkali metal ions and a fixed number of other components like Al, Fe and SiO_2 (Dehghani, 2020). Due to the expandable layer lattice structure and the exchangeability of these cations, there is an increase in basal space as ions and big molecules can pass between the sheets(Du et al., 2020). It has been

documented that big organic molecules can pass through the silicate sheet and align themselves along its plane. They are frequently employed as adsorbents and catalyst supports because of their large surface area and persistent porosity. The physical constitution of montmorillonite particles is commonly observable in sheets and layers. Every layer is made up of two categories of structural sheets: octahedral and tetrahedral. The silicon-oxygen tetrahedral in the tetrahedral sheet is connected to neighboring tetrahedral by sharing three corners, forming a hexagonal structure(Saadi et al., 2015). Each tetrahedron's leftover fourth corner forms a section of the nearby octahedral sheet. Usually, magnesium or aluminum are combined with hydroxyl and oxygen from the tetrahedral sheet in a sixfold coordination to form the octahedral sheet. These two sheets come together to form a layer. In a clay crystallite, interlayer cations, hydrogen bonding, Van der Waals force, and electrostatic force (Dehghani, 2020) can all connect many layers.

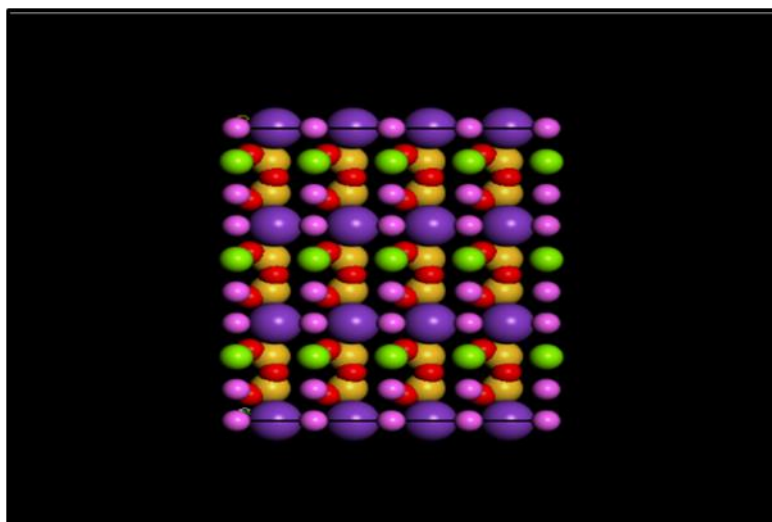


Figure 3-1 Structure of montmorillonite generated using Material Studio Software

Physisorption refers to the process in which adsorbate molecules are drawn towards the adsorbent surface owing to Van de Waals forces under high pressure and can be released when pressure is reduced. Physical adsorption offers several benefits, such as low energy consumption, cost effectiveness, adaptable design, absence of water or other chemicals, safety and ease of operation, and scalability across a broad range of temperatures and pressures. Chemisorption: the gas molecules experience covalent chemical reactions and attach to specific locations on the adsorbent bed. The sharing and movement of valence electrons between the adsorbent and gas

molecules generate more robust covalent bonds, which means that it takes more energy to eliminate them.

3.3. Grand Canonical Monte Carlo Simulation

Grand Canonical Monte Carlo (GCMC) Simulations is a computational technique used in the study of adsorption, gas-liquid equilibrium, surface phenomena, and other systems where particle exchange is important. The Material Studio (2020) Software is built with a GCMC module for modelling and simulating systems, to study the parameters of atoms and molecular structure of the materials(Lasich, 2020). Various changes to the system are performed, at random (another name for random sampling approach is Monte Carlo approach), and for each change there is a probability to accept each change. The energy differential between the new and old configurations determines the likelihood of acceptance of these modifications.

The motion is rejected if the energy change is greater than a predefined tolerance. This makes it possible to calculate a statistical average for numerous states. The GCMC steps for adsorption isotherms contain thousand displacement moves and attempts of either insertion or deletion with equal probability. To ensure equilibration of the system, no less than 2×10^6 moves were used to equilibrate, followed by a further 2×10^7 moves to generate results. Averaging across three independent simulations was undertaken for each data point in the adsorption isotherms, with the standard deviation being used for the estimated uncertainty. Five thousand steps are typically required for the system to reach equilibrium, and additional 5000 steps are used to obtain ensemble averages.

3.4. Simulation Details

The increasing need to enhance the effectiveness and efficiency of biogas upgrading processes has led to the realization that computational approaches are useful instruments for examining various aspects of the process. The field of mathematical modeling and simulation of adsorption-based processes for biogas upgrading has grown significantly in recent years due to advancements in this field. Comparing and evaluating various configurations with computational techniques has become more straightforward than through field testing and laboratory setups. Furthermore, there are still significant technical barriers to the investigation of process dynamics in experimental

approaches(Dehghani, 2020). For instance, it is difficult for the experiments to easily measure some aspects, including how cycle time affects stream pressure and concentration.

Monte Carlo molecular simulations were performed in the grand canonical ensemble and the experimental data was validated using previous laboratory experiments. The purpose of the simulations was to forecast the adsorption of nitrogen, sulfur dioxide, carbon dioxide, methane, and ethane on a montmorillonite lattice. Adsorption isotherms were produced for both pure species and a gas mixture that contained hydrogen sulfide as the remaining component and 65 mol% methane, 15 mol% nitrogen, 10 mol% ethane, and 5 mol% carbon dioxide.

The selection of a forcefield, which reasonably accurately depicts the potential energy surface of all classes of molecules, is an essential component of any simulation. The choice of forcefield will depend on the kind of structure being studied, as forcefields are typically adjusted for certain groupings of systems. Simulation can either be conducted using: Forcite, Polymorph, Morphology, Sorption, Amorphous Cell, and Adsorption Locator can be used with the COMPASS, pcff, cvff, Dreiding, and Universal forcefields(Dehghani, 2020). COMPASS forcefield was selected for this study due to their wide variety of molecules and polymers, it is the first and only forcefield that permits precise and simultaneous prediction of gas-phase properties (structural, conformational, vibrational, and so on) and condensed-phase properties (equation of state, cohesive energies, and so on).

The Ewald technique (Dehghani, 2020) is a method for the computation of non-bond energies in periodic systems. With the Ewald technique, you can choose the computation's accuracy level before the calculation is performed. Since it is challenging to estimate the cutoff and convergence constants(Dehghani, 2020), a feature that automatically determines these values to a predetermined degree of precision is offered instead. An atom-based calculation with a large cutoff (19 Å) over the measured range can perform comparably to an Ewald calculation with accuracy=10⁻⁴, depending on the system. For the dispersive van der Waals interactions, a cut-off radius of 1.85 nm with an analytical tail correction was utilized, and for the electrostatic interactions, the Ewald summation method was applied.

Adsorption Isotherm can be obtained by gathering the average loading at equilibrium at each pressure or fugacity point. Millions of random moves are made in each simulation by the sample-chosen ensemble. The standard Metropolis technique handles these arbitrary Monte Carlo motions, which are allowed or rejected depending on a weighting of the energy akin to

Boltzmann's (Dehghani, 2020). A set of sample configurations is produced by the stochastic Metropolis method from a given ensemble, and these configurations can be used to compute average thermodynamic properties. Adsorption of gas into random movements that imitate real-world behavior is applied to the system; changes in the system's potential energy determine whether the motion is accepted or rejected. The details of the Metropolis schemes are the basis for Markov chain Monte Carlo methods from which a class of algorithms sampling from a probability distribution based on constructing of Markov chain that has the desired distribution as its equilibrium distribution.

The gas particles underwent the following manipulations (probabilities of occurrence are shown in parenthesis: Exchange (39%), conformer (20%), rotation (20%), translation (20%), and regrowth (2%) (Dehghani, 2020). The remaining movements simulate the thermal motion of the adsorbed molecules within the montmorillonite lattice, while the first two movements mimic adsorption and desorption, respectively. This allows the parameters of the model to be determined, such as the maximum adsorption capacity of the adsorbent and the strength of the interaction between the impurity and the adsorbent. In the experimental procedure, a virtual model of Montmorillonite was created and incorporated into a biogas purification system.

While regeneration is carried out at a significantly lower pressure, allowing the impurities to desorb back to the gas phase and be removed from the bed, the pressure during the adsorption step is maintained at the highest level to increase the adsorbed number of impurities, leading to enrichment of product component in the gas phase. The proposed research is to determine optimal operating conditions of pressure swing adsorption column that uses montmorillonite lattice, which operates at ambient temperature. Each Monte Carlo simulation run represented a single iteration of biogas purification. For each run, the purity of the resulting biogas was recorded, alongside the

exact input parameters used. This process was repeated thousands of times, with different randomly selected input parameters for each run.

- All species were simulated over the fugacity range of $1-1 \times 10^3$ kPa and constant temperature of $T = 298$ K.
- Each production run was set at 10,000,000 Monte Carlo moves (as before), to ensure that adequately representative statistics would be obtained for the system being analyzed.
- Three independent simulations for each species to generate as many data points as needed to describe the behavior at different pressure.
- The production run was repeated for each species in order to generate enough data to reduce statistical uncertainty.
- The second equilibration step began when each phase reached equilibrium. To do this, the simulation had to be repeated until there were no more compositional changes for each phase and the compositions had stabilized at their corresponding average values.

3.5. Adsorption Isotherms

An adsorption isotherm mathematically defines the relationship between the concentration of the molecules of a given species in the gas phase with its concentration in the adsorbed phase, under equilibrium conditions and constant temperature. The adsorption isotherm can be obtained by collecting the average loading at equilibrium at each pressure or fugacity point (Saadi et al., 2015). To employ the fitted models in later process modeling calculations, the adsorption isotherm modeling was carried out, the results are presented in Appendix-A. Several suppositions underline this explanation of adsorption: Adsorption site equivalency, adsorbed molecules' immobility, single-site occupancy, surface homogeneity, and the absence of adsorbate molecule interactions.

All pure species adsorption isotherms were assessed in terms of the most widely used two-parameter adsorption isotherm models, namely those of Langmuir, Freundlich and Redlich-Peterson (Dehghani, 2020). The Langmuir isotherm provides a quantitative framework for analyzing experimental data, which determine the important parameters such as the adsorption capacity and the affinity of the adsorbate for the adsorbent and compare the adsorption characteristics of different adsorbents or surfaces. Mathematically, the Langmuir model relationship given as:

$$q = \frac{q_0 b P}{1 + b P} \quad \text{Equation 3.1}$$

where P is the gas reservoir pressure, b is the Langmuir equilibrium constant, q_0 is the highest amount of gas absorbed by the adsorbent, and q is the amount of gas adsorbed. Either pressure or fugacity can be used to convey this statement.

The Freundlich model accounts for reversible and non-ideal adsorption, while also factoring in non-uniform distribution of adsorption affinities and heats across heterogeneous surfaces. It is presented as:

$$q = K_f P^{\frac{1}{n}} \quad \text{Equation 3.2}$$

where K_f is the Freundlich constant describing adsorption capacity and $1/n$ represents the degree of heterogeneity of the surface.

The Redlich-Peterson isotherm is a hybrid isotherm that incorporates features of both the Langmuir and Freundlich approaches; at low pressures it resembles the Langmuir model while at high pressures it approaches the Freundlich isotherm, as given by:

$$q = \frac{K_g P}{1 + a R P B_s} \quad \text{Equation 3.3}$$

in which K_g/aR indicates the adsorption capacity while B_s is a constant indicating deviation from the simplistic Langmuir description (for which $B_s = b=1$).

Using the root-mean-square error (RMSE) as the objective function for minimization, the Langmuir equation was fitted to the molecular simulation findings. For the molecular simulations, the Peng–Robinson cubic equation of state was utilized to translate between pressure and chemical potential [76]. This is one of the best two-constant cubic equations of state and is commonly used in natural gas processing and related chemical engineering fields:

$$RMSE = \left(\sum \frac{(q_{fit} - q_{sim})^2}{p} \right)^{\frac{1}{2}} \quad \text{Equation 3.4}$$

where p is the total number of data points per isotherm, q_{fit} is the fitted uptake of gas, and q_{sim} is the outcome of the molecular simulations.

3.6. Batch Equilibrium Modelling

The computer program Octave (GNU) was undertaken to demonstrate the equilibrium approach, which described system performance of the unchanging amount of montmorillonite in a realistic setting approximating the conditions of a PSA unit for upgrading biogas. This approach requires adsorption isotherm data generated by the Monte Carlo molecular simulations and yields macro-scale results of adsorption system performance in terms of outlet gas compositions, using feed gas composition, operating pressure values, and system temperature as specified inputs.

To determine the yields of the final product gas, material balances for the adsorption and desorption stages yield the adsorbed quantities were carried out for each species in the solid and gas phases. Batch equilibrium experiments are essential for validating adsorption isotherm models. By comparing experimental data to various isotherm models (e.g., Langmuir, Freundlich or Redlich)(Lasich, 2020), it can help to determine which model best fits the adsorption behavior of the system. Batch experiments can be extended to study the kinetics of adsorption, helping to understand how fast the adsorption process reaches equilibrium(Dehghani, 2020). This is crucial for designing adsorption processes with the desired efficiency to optimize process parameters such as adsorbent dose, contact time, temperature, and initial concentration of the adsorbate to achieve the desired adsorption efficiency. Table 3.1 presents feed composition and simulation parameters used for generating Adsorption Isotherm for each component of Biogas stream.

Table 3-1 Feed composition and simulation parameters

Species	Feed composition (% mol)	Temperat ure(K)	Pressure(kPa)	Mass(g)
CH ₄	0.65	298K	0.01-1000	
N ₂	0.15	298K	0.01-1000	
C ₂ H ₆	0.10	298K	0.01-1000	
CO ₂	0.05	298K	0.01-1000	
H ₂ S	0.05	298K	0.01-1000	
Montmorillonite				4468g

CHAPTER 4- RESULTS AND DISCUSSIONS

4.1. Introduction

The section discusses the outcomes of the synthesizing and characterization MMT as natural adsorbent for removal of CO₂ in the biogas stream. Also evaluated using at what operating conditions of the PSA system does MMT remove the impurities from biogas. Results obtained in terms of Adsorption Isotherm performances and adsorption capacity compared and discussed. Furthermore, highlights of the experimental data evaluation via Batch equilibrium modeling and the fitted models using RSM are also presented.

4.2. Results

The preferred gas is preferentially adsorbed at high pressure on a porous adsorbent, and the gas is then recovered at low pressure in the PSA process. The amount of impurity removed by adsorption can be described by an adsorption isotherm, which is a relationship between the concentration of the impurity in the gas phase and the amount of impurity adsorbed onto the surface of the adsorbent.

The simulations were validated and compared with reference papers (Khajuria, 2011) and (Dittmer, 2021). Adsorption isotherm calculations can be used to model the behavior of biogas purification systems that use adsorption as a method of removing impurities (Dehghani, 2020).

4.3. Discussion

Adsorption isotherms generated for all the species of interest in this study. Simulation parameters are presented in Table 3.1. The results are the average of three independent simulations and calculated standard deviation for each fugacity value. Where f is the gas fugacity and q are the amount of gas adsorbed into the solid. The adsorption capacity was found to be low at low fugacity pressure, but as the pressure increases, all species are adsorbed into the montmorillonite adsorbent bed, Figure 4.1 also indicates how each species preferential adsorbed in the bed. At high pressures, most of the species turns to get saturated. Both axes have been made logarithmic for clarity. Note that the absolute adsorptions are shown in Table 4.1 to 4.5. Graphical results for Table 4.1 to 4.5 are presented in Appendix A.

Table 4-1 Adsorption isotherm for CH₄ at 298K and 1.0 x10⁻³ to 1.0 x10³ kPa.

Fugacity (kPa)	Average	Standard deviation
1.0 x10 ⁻³	1.29 x10 ⁻⁸	3.02 x10 ⁻¹⁰
1.47 x10 ⁻²	1.86 x10 ⁻⁷	2.72 x10 ⁻⁹
2.15 x10 ⁻¹	2.71 x10 ⁻⁶	1.64 x10 ⁻⁸
3.16	3.95 x10 ⁻⁵	9.27 x10 ⁻⁸
4.64 x10 ¹	5.57 x10 ⁻⁴	1.64 x10 ⁻⁶
6.81 x10 ²	4.51 x10 ⁻³	1.26 x10 ⁻⁵
1.0 x10 ³	1.04 x10 ⁻²	1.45 x10 ⁻⁵

Table 4-2 Adsorption isotherm for C₂H₆ at 298K and 1.0 x10⁻³ to 1.0 x10³ kPa.

Fugacity (kPa)	Average	Standard deviation
1.0 x10 ⁻³	1.73 x10 ⁻⁷	3.49 x10 ⁻⁹
1.46 x10 ⁻²	2.53 x10 ⁻⁶	1,11 x10 ⁻⁸
2.15 x10 ⁻¹	3.74 x10 ⁻⁵	2.76 x10 ⁻⁷
3.16	5.57 x10 ⁻⁴	2.14 x10 ⁻⁶
4.64 x10 ¹	4.24 x10 ⁻³	4.32 x10 ⁻⁶
6.81 x10 ³	5.96 x10 ⁻³	3.73 x10 ⁻⁵
1.0 x10 ³	9.99 x10 ⁻³	1.91 x10 ⁻⁴

Table 4-3 Adsorption isotherm for N₂ at 298K and 1.0 x10⁻³ to 1.0 x10³ kPa.

Fugacity (kPa)	Average	Standard deviation
1.0 x10 ⁻³	1.09 x10 ⁻⁹	7.45 x10 ⁻¹¹
1.47 x10 ⁻²	1.87 x10 ⁻⁸	1.48 x10 ⁻⁹
2.15 x10 ⁻¹	2.86 x10 ⁻⁷	3.66 x10 ⁻⁹
3.16	4.22 x10 ⁻⁶	2.55 x10 ⁻⁹
4.64 x10 ¹	6.16 x10 ⁻⁵	158 x10 ⁻⁷
6.81 x10 ²	8.07 x10 ⁻⁴	1.42 x10 ⁻⁶
1.0 x10 ³	4.85 x10 ⁻³	9.92 x10 ⁻⁶

Table 4-4 Adsorption isotherm for CO₂ at 298K and 1.0 x10⁻³ to 1.0 x10³ kPa.

Fugacity (kPa)	Average	Standard deviation
1.0 x10 ⁻³	4.67 x10 ⁻⁹	4.42 x10 ⁻¹⁰
1.47 x10 ⁻²	7.20 x10 ⁻⁸	1.41 x10 ⁻⁹
2.15 x10 ⁻¹	1.06 x10 ⁻⁶	1.35 x10 ⁻⁸
3.16	1.53 x10 ⁻⁵	7.84 x10 ⁻⁸
4.64 x10 ¹	2.19 x10 ⁻⁴	1.42 x10 ⁻⁶
6.81 x10 ²	2.24 x10 ⁻³	7.22 x10 ⁻⁶
1.0 x10 ³	6.50 x10 ⁻³	1.82 x10 ⁻⁵

Table 4-5 Adsorption isotherm for H₂S at 298K and 1.0 x10⁻³ to 1.0 x10³ kPa.

Fugacity (kPa)	Average	Standard deviation
1.0 x10 ⁻³	1.49 x10 ⁻⁸	1.09 x10 ⁻⁹
1.47 x 10 ⁻²	2.11 x10 ⁻⁷	5.25 x10 ⁻⁹
2.15 x10 ⁻¹	3.0 x10 ⁻⁶	1.85 x10 ⁻⁸
3.16	4.53 x10 ⁻⁵	1.04 x10 ⁻⁷
4.64 x10 ¹	6.35 x10 ⁻⁴	5.24 x10 ⁻⁷
6.81 x10 ²	4.71 x10 ⁻³	1.03 x10 ⁻⁵
1.0 x10 ³	1.03 x10 ⁻²	1.03 x10 ⁻⁵

The tables present adsorption capacity for each species at different pressures. The results show how much gas adsorbed as pressure increases. Even though the trend is not linear, there may be steric effects related to the size and shape of gas molecules as well as the size and shape of channels within MMT lattice.

Comparing the magnitudes of the diffusivities yields the following ranking in terms of rates of diffusion in the MMT: H₂S>N₂>CO₂>C₂H₆>CH₄. The ranking of affinities in terms of adsorption (considering pressures from 1.0 kPa upwards) is H₂S>CO₂>O₂>N₂>CH₄>C₂H₆. Comparing these two rankings as well as the results in Figure 4.1 suggest that it may not be straightforward to predict the diffusion of biogas constituents in MMT based solely on the quantity of gas adsorbed or a simplistic measure such as a single molecular property.

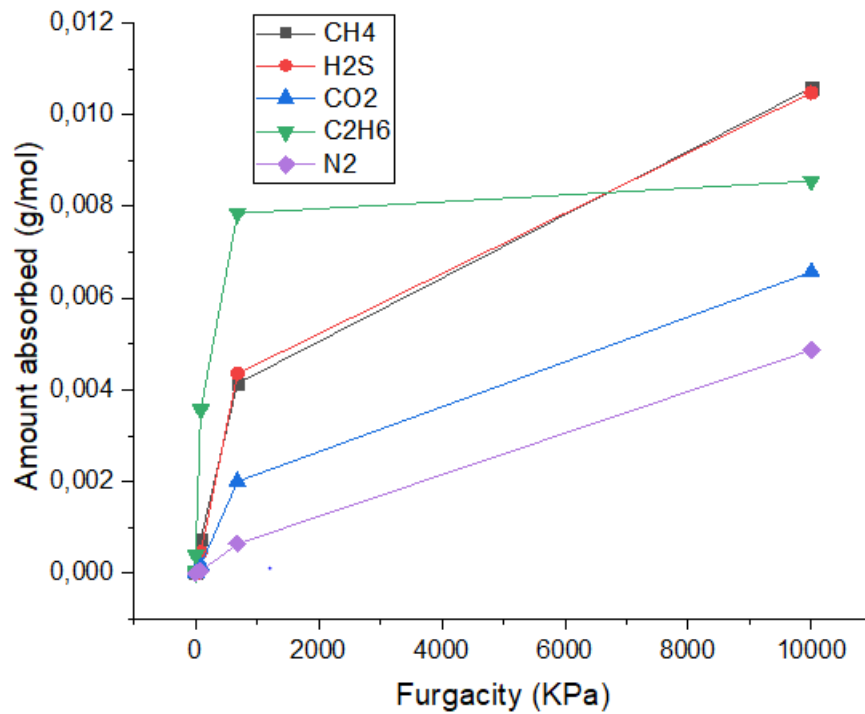


Figure 4-1 Amount of gas adsorbed into the solid q and fugacity f of the gas.

The following graph gives a more detailed description that shows at what pressure each species behaves at a given pressure. The graph indicates that CH_4 , CO_2 and H_2S are adsorbed into montmorillonite bed at a pressure above 10kPa, however C_2H_6 is preferentially adsorbed at a very low pressure and becomes saturated at high pressure above 1×10^3 kPa. Since CO_2 and H_2S are the main components that need to be removed, the results show that the adsorbent is effective enough for PSA system. Although it might be difficult to separate C_2H_6 and CH_4 under the same condition since C_2H_6 is preferentially adsorbed due to combination of larger size, linear shape, and higher polarizability makes it more prone to adsorption at lower pressures compared to other species. In the context of adsorption isotherms, the standard deviation can be used to assess the goodness of fit of a particular adsorption model to the experimental data. If the standard deviation is high, it suggests that there is a lack of good model-data that fit the adsorption behavior. and may not be suitable for predicting adsorption behavior. On the other hand, if the standard deviation is low, it suggests that the model provides a good fit to the data and can be used to predict adsorption behavior with reasonable.

The Sum of Squares Error (SSE) states the deviation between the experimental results and the values predicted by the isotherm models. It was calculated for each gas component as follows: the measured and model predicted values of the amount adsorbed, respectively, and n represents

the number of experimental data points fitted for each experiment. The fitted parameters for Langmuir, Freundlich and Redlich-Peterson (i.e., Q_0 and K), SSE values, and correlation coefficients are presented in Table 4.6 to 4.8.

Table 4-6 Fitted Langmuir Adsorption Mode Parameters Q_0 along with the Sum-Square Error (SSE) and the Correlation Coefficient (R^2)

Species	SSE	R^2	Q_0	B
CH₄	1.80×10^{-7}	0.99	7.79×10^{-4}	7.79×10^{-4}
CO₂	6.70×10^{-8}	0.99	7.89×10^{-3}	4.99×10^{-4}
C₂H₆	6.13×10^{-6}	0.96	8.61×10^{-3}	1.52×10^{-2}
H₂S	1.81×10^{-7}	0.99	1.17×10^{-2}	8.72×10^{-4}
N₂	2.84×10^{-8}	0.99	9.42×10^{-3}	1.07×10^{-4}

Table 4-7 Fitted Freundlich Adsorption Mode Parameters and K along with the Sum-Square Error (SSE) and the Correlation Coefficient (R^2)

Species	SSE	N	R^2	K_f
CH₄	4.91×10^{-5}	11.42	0.89	2.50×10^{-3}
C₂H₆	3.59×10^{-5}	12.39	0.96	3.14×10^{-3}
CO₂	1.05×10^{-5}	6.42	0.93	1.00×10^{-3}
H₂S	4.78×10^{-5}	11.48	0.89	2.52×10^{-3}
N₂	7.64×10^{-6}	5.27	0.90	7.85×10^{-4}

Table 4-8 Fitted Redlich -Peterson Adsorption Mode Parameters aR, Bs, Kg and the Correlation Coefficient (R²)

Species	Bs	aR	R ²	Kg
CH ₄	9.19 x10 ⁻¹	2.43 x10 ⁻³	1.00	1.31 x10 ⁻⁵
CO ₂	8.61 x10 ⁻¹	2.91 x10 ⁻³	0.99	5.92 x10 ⁻⁶
C ₂ H ₆	8.49 x10 ⁻¹	1.93 x10 ⁻¹	0.99	4.75 x10 ⁻⁴
H ₂ S	8.61 x10 ⁻¹	2.91 x10 ⁻³	0.99	9.72 x10 ⁻⁶
N ₂	8.61 x10 ⁻¹	2.91x10 ⁻³	0.98	4.17 x10 ⁻⁶

The adsorption model equation data presented from the Tables was successful in all cases, with correlation coefficients (R²) being no less than 0.99 for all species for the Langmuir Adsorption model. The results obtained from experimental isotherm and calculated standard deviation across all three models which show inconsistent on the correlation co-efficient from Freundlich and Relich-Peterson as shown in Table 4.9.

Table 4-9 Comparison between different fitted models of Biogas species.

Species	Langmuir		Redlich-Peterson		Freundlich	
	R ²	Absolute Deviation (%)	R ²	Absolute Deviation (%)	R ²	Absolute Deviation (%)
CH ₄	0.99	20.17	1.00	1.79	0.89	1.65 x10 ⁶
CO ₂	0.99	15.08	0.99	14.99	0.92	1.16 x10 ⁶
C ₂ H ₆	0.98	23.39	0.99	87.12	0.96	1.62 x10 ⁵
N ₂	0.99	17.44	0.98	174.86	0.90	3.07 x10 ⁶
H ₂ S	0.99	22.23	0.89	22.33	0.99	1.45 x10 ⁶

This concluded that Langmuir provided a good fit for adsorption isotherm model of the PSA system. Hence, the optimal model to select in terms of both agreeing with the results and minimizing overfitting is Langmuir model. In terms of fitting adsorption isotherm model, it may be preferable to select either Langmuir or Redlich-Peterson, purely on the basis of R² as a value for comparison.

4.4. Batch Equilibrium Modelling

The equilibrium modeling was conducted using GNU Octave tool. The adsorption system was modeled using a batch equilibrium technique (Dittmer, 2021), which represented the system as a cycle with a constant amount of solid adsorbent. Material balances for the adsorption and desorption stages produce the adsorbed amounts of each species in the solid and gas phases, and solving these balances yields the final product composition. Modelling of PSA was conducted at ambient temperature (298K) and atmospheric pressure (101.325kPa), biogas composition of 65% CH₄, 15% C₂H₆, 10% N₂, 5% CO₂ and 5% H₂S. The adsorbed amounts of each species in the solid and gas phases are determined by equilibrium stages of adsorption and desorption, and the ultimate product composition is obtained by solving these balances. Due to selective adsorption of CO₂ by MMT, the gas discharged of the pressure swing adsorption unit described by Equations 4.1 to 4.3 which would contain rich CH₄.

$$n_i^{in} = n_i^{out} + q_i^{ad} \quad \text{Equation 4.1}$$

$$q_i = \frac{a_i P_i W}{1 + \sum b_i P_i} \quad \text{Equation 4.2}$$

$$n_i^{in} = n_i^{out} + \frac{W b P q_i}{1 + b P} \quad \text{Equation 4.3}$$

where q_i is the amounts of component i in the bulk-gas adsorbed at equilibrium, n_i^{in} and n_i^{out} are the number of moles for component i fed and out respectively. P_i is the partial pressure at adsorption equilibrium, W is the mass of adsorption bed and b_i is the Langmuir constants. Table 4.9 Present the amount of gas accumulated in adsorption bed at equilibrium. Material balance was conducted for the feed stream and outlet stream using equation 4.1 to 4.3, sample of calculation is presented in Appendix C.

Table 4-10 Overall bed mass (W) of the PSA system at 298K and 101.325kPa

CH₄(g/mol)	C₂H₆(g/mol)	H₂S (g/mol)	N₂ (g/mol)	CO₂ (g/mol)
5.24 x10 ⁻⁷	6.41 x10 ⁻⁵	7.54 x10 ⁻⁷	6.81 x10 ⁻⁸	2.17 x10 ⁻⁶
7.69 x10 ⁻⁶	9.41 x10 ⁻⁴	1.11 x10 ⁻⁵	9.99 x10 ⁻⁷	3.19 x10 ⁻⁵
1.13 x10 ⁻⁴	1.38 x10 ⁻²	1.62 x10 ⁻⁴	147 x10 ⁻⁵	4.69 x10 ⁻⁴
1.66 x10 ⁻³	2.03 x10 ⁻¹	2.39 x10 ⁻³	2.15 x10 ⁻⁴	6.88 x10 ⁻³
2.45 x10 ⁻²	2.99	3.52 x10 ⁻²	3.18 x10 ⁻³	1.01 x10 ⁻¹
3.92 x10 ⁻¹	1.69 x10 ¹	5.50 x10 ⁻¹	5.03 x10 ⁻²	1.57
8.10	1.41 x10 ¹	9.99	8.87 x10 ⁻¹	7.86

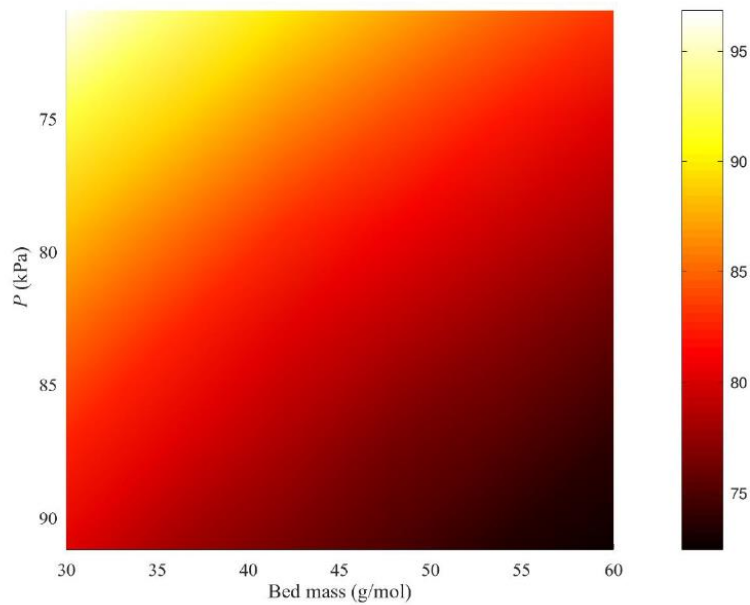


Figure 4-2: Heat map of the overall biogas component in the outlet stream of PSA system as a function of adsorbent quantity and operating pressure ratio.

The colors indicate the high and low values of the bed at different pressures, ideally the optimal operating at this point would be at a lower pressure which would also minimize the cost of running the system at high pressure. To replicate process conditions in the literature as closely as possible for the purposes of obtaining PSA conditions, a bed mass of about 30-39 g/mol of feed gas with an operating pressure of approximately 70-82 kPa would be suitable for cleaning a gas mixture

consisting of 65 mol-% methane with carbon dioxide. These conditions can yield a methane-rich stream comprising 96 mol-% methane and all the methane that was in the feed, demonstrating that MMT in a PSA system can be used for upgrading biogas. It was noted that the secondary outlet stream produced two gas streams, one consisting solely of carbon dioxide, and another comprising about 93-96 mol-% CH_4 . Therefore, the proposed PSA employing MMT as the adsorbent may satisfy the requirements of this biogas upgrading.

It was be noted that test calculations were performed for operation approaching 1000 kPa, however the magnitude of methane uptake into MMT meant that achieving both outlet composition specifications i.e. one gas stream with 100 mol-% CO_2 and another with a stream more than 96 mol-% CH_4 would be challenging in practice when employing a single stage pressure swing adsorption system. With reference to CO_2 removal, it is also then clear that very small bed sizes may be sufficient to produce purified biogas. Figure 4.3 presents the operating range yields performance such that the targeted methane content of 93-96 mol-% is achievable.

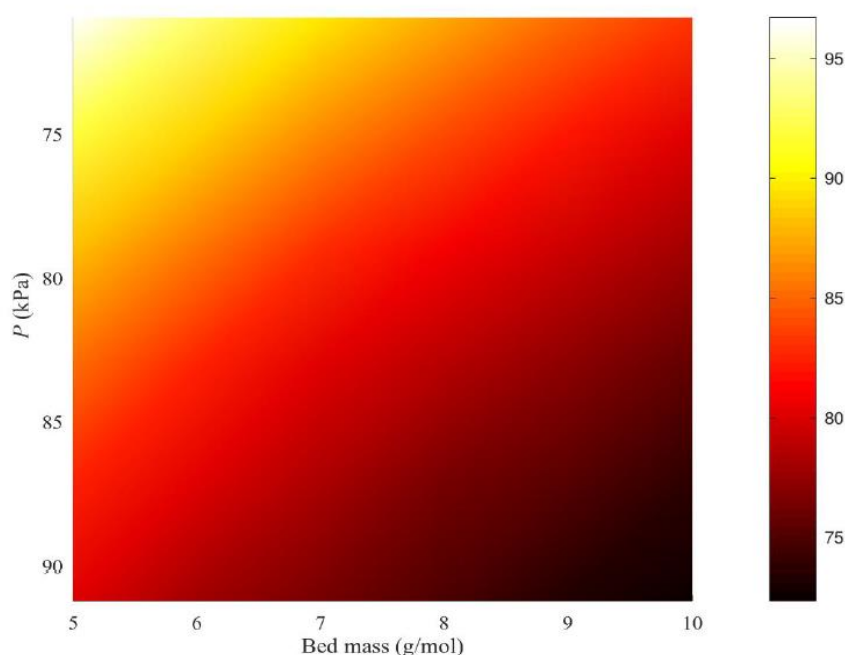


Figure 4-3 Heat map of the overall biogas component in the outlet stream of PSA system as a function of adsorbent quantity and operating pressure ratio.

The required bed size in this case is about 5-6 g/mole of feedstock. Therefore, when considering this correction factor to account for consistent deviations between available experimental data and the predictions of the COMPASS forcefield, it is apparent that MMT can serve as a suitable adsorbent for the biogas upgrading process.

In addition, for the PSA system performance can be evaluated if the separation was reached. The batch equilibrium model makes it simple to develop this relationship, which may then be utilized as a true separation factor for the PSA system(Dittmer, 2021). Equation can be used to indicate a new separation factor for the PSA system if it is defined as the mole fractions of two components in the product divided by the ratio in the feed.4.5 shows. The graphical results are presented in Appendix C.

$$\alpha = \frac{\frac{C_{ch_4in}}{C_{ch_4out}}}{\frac{C_{CO_2}}{C_{ch_4out}}} \quad \text{Equation 4.4}$$

The calculated separation factor was found to be greater than one: $\alpha = 13$, which indicates separation process was effective as removal CO_2 and enrichment of CH_4 was achieved.

The batch equilibrium model is simple and effective for analyzing PSA systems, with accurate results. Although it cannot anticipate the performance of kinetically controlled systems, it can serve as a screening tool for adsorbent selection and process comparisons during the early design stage of PSA systems.

CHAPTER 5-CONCLUSIONS AND RECOMMENDATIONS

The study focused on investigating the suitability of montmorillonite as a novel adsorbent for biogas purification. This will be accomplished by using Monte Carlo simulations in the grand canonical ensemble simulation to develop adsorption isotherms, along with macro-scale batch equilibrium modeling. This chapter summarizes the key results and makes recommendations for future research and decision-making.

The specific objectives were:

1. To determine the effectiveness of montmorillonite as a biogas purifier.
2. To Establish the optimal operating condition of a Pressure Swing Adsorption (PSA) system using montmorillonite.

5.1. Conclusion

The outlined methodology, focused on the simulation-based assessment of the novel adsorber's effectiveness, provides a rigorous and reliable framework to investigate our research question. The results of this research, which are detailed in subsequent chapters, offer valuable insights into the potential of the novel adsorber in biogas purification. Monte Carlo molecular simulations were performed in the grand canonical ensemble to predict adsorption of carbon dioxide, methane, hydrogen sulfide, ethane, and nitrogen on montmorillonite lattice.

Adsorption isotherms were produced for both pure species and a gas mixture that mimicked actual natural gas fields by including 65% methane, 15% nitrogen, 10% ethane, 5% carbon dioxide, and the remaining hydrogen sulfide. The gas mixture's settings of interest, which included 293 K and 0.01–1000 kPa of pressure, were representative of real-world circumstances. This study showed that montmorillonite might be a practical adsorbent for pressure-swing adsorption, which is a sorption procedure used to specifically remove CO₂ and H₂S.

There is a high correlation between the simulated results and the reported values in papers as shown in figure 3.2 and 4.1 With respect to the other species under consideration (i.e., nitrogen, oxygen, methane, hydrogen, and carbon dioxide), commonly used adsorption isotherm models adequately described the observed sorption behaviour.

Simulations of mixture adsorption were also undertaken, for which it was observed that optimal removal of non-calorific components (CO_2 , H_2S) occurred at high pressure (specifically at 10 kPa, the lowest pressure considered in this study). The strong selectivity of the montmorillonite adsorbent in favour of carbon dioxide at low pressures suggests that future experimental work may yield a practicable PSA system to produce cleaner-burning biogas free from impurities and with a reduced non-calorific content. Montmorillonite was successfully functionalized with its cations exchange methods and gas adsorption capabilities under varied temperature and pressure.

In addition, the batch equilibrium modelling was undertaken with a view to assessing the feasibility of montmorillonite as an adsorbent for PSA separation of biogas and at what conditions does the PSA operate at optimal. The operating condition obtained was at a pressure of 70-82 kPa and 30-39g/mol of bed mass. This was undertaken within the context of biogas upgrading process, where the effects of operating pressure and bed size for a PSA system were achievable. It was demonstrated that this unit may be incorporated into biogas reforming process, as it can meet the requirements of the biogas feed preparation step in terms of separation power.

PSA is a complex process, since process control, yield and purity of the product that are difficult to maintain as compared to other upgrading technologies. The selection of optimal design and operating parameters is a difficult task due to highly complex and tough design procedure of transference singularities of adsorbate in adsorption column and extreme computational requirements to reach the steady cyclic state between the sequences. Due to the design of PSA system and the arrangement of adsorption columns and cycle sequences, the adsorption capacity performance can be affected and that might lead to low recovery of CH_4 . This has been a major drawback of PSA especially in comparison to other biogas upgrading technologies like amine scrubbing since a substantial amount of CH_4 gets discharged with the off gas.

5.2. Recommendations

Pressure swing operation does of course entail its own challenges, such as higher capital costs for implementation and a techno-economic assessment that balances capital and operating costs to determine the optimal pressure would be necessary. Adsorption typically entails low energy costs compared to many separation schemes, and it can therefore be helpful to consider montmorillonite in the pressure swing adsorption system for the purpose of biogas upgrading.

It could be advantageous to investigate additional adsorbents that can be used to upgrade or improve renewable producer gases, particularly those that can be generated in peri-urban and rural settings. To have the most possible influence on boosting energy availability in emerging and underdeveloped nations and regions, special attention should be paid to adsorbents that are easily accessible in these locations. Exploring the blending of unmodified adsorbents with high-performance materials like MMT, MOFs and CMSs in a layered system to reduce adsorbent preparation costs and improve interconnection between the adsorbate and adsorbent surface to enhance adsorption capacity of the adsorbent.

MMT may be incorporated into biogas reforming processes for the removal of carbon dioxide from feedstock as part of biogas upgrading; for the purposes of development due to its recent active reference study. Emerging frontiers in this field encompass advancements in computational modelling and simulation for predictive PSA performance optimization, the exploration of hybrid separation methodologies combining PSA with other techniques like membranes or cryogenic distillation, and the integration of renewable energy sources to power the purification processes, fostering a more sustainable and efficient biogas upgrading landscape. Improve and modify of existing PSA system designs like exploration of composite materials and diverse bed configurations. Explore hybrid upgrading processes to achieve high purity of CH₄ and CO₂ recovery from the biogas stream while controlling CH₄ and PSA step. Address the gap concerning the environmental life cycle of PSA systems, emphasizing the need for comprehensive analyses in future studies.

REFERENCES

- ABD, A., OTHMAN, M., NAJI, S. & HASHIM, A. 2021. Methane enrichment in biogas mixture using pressure swing adsorption: process fundamental and design parameters. *Materials Today Sustainability*, 11, 100063.
- ABDESHAHIAN, P., LIM, J. S., HO, W. S., HASHIM, H. & LEE, C. T. 2016. Potential of biogas production from farm animal waste in Malaysia. *Renewable and Sustainable Energy Reviews*, 60, 714-723.
- ABDUL, D., WENQI, J. & TANVEER, A. 2022. Environmental stewardship: Analyzing the dynamic impact of renewable energy, foreign remittances, and globalization index on China's CO₂ emissions. *Renewable Energy*, 201, 418-425.
- ACHINAS, S., ACHINAS, V. & EUVERINK, G. J. W. 2017. A technological overview of biogas production from biowaste. *Engineering*, 3, 299-307.
- AHMED, S. F., MOFIJUR, M., TARANNUM, K., CHOWDHURY, A. T., RAFA, N., NUZHAT, S., KUMAR, P. S., VO, D.-V. N., LICHTFOUSE, E. & MAHLIA, T. 2021. Biogas upgrading, economy and utilization: a review. *Environmental Chemistry Letters*, 19, 4137-4164.
- AMIGUN, B. & VON BLOTTNITZ, H. 2009. Capital cost prediction for biogas installations in Africa: Lang factor approach. *Environmental Progress & Sustainable Energy: An Official Publication of the American Institute of Chemical Engineers*, 28, 134-142.
- AWE, O. W., ZHAO, Y., NZIHO, A., MINH, D. P. & LYCZKO, N. 2017. A review of biogas utilisation, purification and upgrading technologies. *Waste and Biomass Valorization*, 8, 267-283.
- AZIZIAN, S. & ERIS, S. 2021. Adsorption isotherms and kinetics. *Interface science and technology*. Elsevier.
- BAENA-MORENO, F. M., RODRÍGUEZ-GALÁN, M., VEGA, F., VILCHES, L. F., NAVARRETE, B. & ZHANG, Z. 2019. Biogas upgrading by cryogenic techniques. *Environmental Chemistry Letters*, 17, 1251-1261.
- BAHRUN, M. H. V., BONO, A., OTHMAN, N. & ZAINI, M. A. A. 2022. Carbon dioxide removal from biogas through pressure swing adsorption—A review. *Chemical Engineering Research and Design*, 183, 285-306.
- BERNARDO, P. & CLARIZIA, G. 2013. 30 years of membrane technology for gas separation. *Chem. Eng.*, 32, 1999-2004.
- BRUNETTI, A., SCURA, F., BARBIERI, G. & DRIOLI, E. 2010. Membrane technologies for CO₂ separation. *Journal of Membrane Science*, 359, 115-125.

- CAVAIGNAC, R. S., FERREIRA, N. L. & GUARDANI, R. 2021. Techno-economic and environmental process evaluation of biogas upgrading via amine scrubbing. *Renewable Energy*, 171, 868-880.
- CHOI, B. S., PARK, G. I., KIM, J. H., LEE, J. W. & RYU, S. K. 2001. Adsorption equilibrium and dynamics of methyl iodide in a silver ion-exchanged zeolite column at high temperatures. *Adsorption*, 7, 91-103.
- CLA, T. O. S. Swelling Clays as Components of the Engineered Barrier System for Geological Repositories.
- COZMA, P., WUKOVITS, W., MĂMĂLIGĂ, I., FRIEDL, A. & GAVRILESCU, M. 2015. Modeling and simulation of high pressure water scrubbing technology applied for biogas upgrading. *Clean Technologies and Environmental Policy*, 17, 373-391.
- DAHUNSI, S. O., FAGBIELE, O. O. & YUSUF, E. O. 2020. Bioenergy technologies adoption in Africa: a review of past and current status. *Journal of cleaner production*, 264, 121683.
- DAMYANOVA, S. & BESCHKOV, V. 2020. Biogas as a source of energy and chemicals. *Biorefinery Concepts, Energy and Products*, 1-14.
- DAS, J., RAVISHANKAR, H. & LENS, P. N. 2022. Biological biogas purification: Recent developments, challenges and future prospects. *Journal of Environmental Management*, 304, 114198.
- DAVARPANA, M., HASHISHO, Z., CROMPTON, D., ANDERSON, J. E. & NICHOLS, M. 2020. Modeling VOC adsorption in lab-and industrial-scale fluidized bed adsorbers: Effect of operating parameters and heel build-up. *Journal of Hazardous Materials*, 400, 123129.
- DEHGHANI, M. H., YETILMEZSOY, K., SALARI, M., HEIDARINEJAD, Z., YOUSEFI, M. AND SILLANPÄÄ, M. 2020. Adsorptive removal of cobalt (II) from aqueous solutions using multi-walled carbon nanotubes and γ -alumina as novel adsorbents: Modelling and optimization based on response surface methodology and artificial neural network. *Journal of Molecular Liquids*, 299, 112154.
- DITTMER, C., KRÜMPEL, J., & LEMMER, A. 2021. Modeling and Simulation of Biogas Production in Full Scale with Time Series Analysis. *Microorganisms*, 9, 324.
- DRIOLI, E., BRUNETTI, A. & BARBIERI, G. 2011. Ceramic membranes in carbon dioxide capture: applications and potentialities. *Advances in Science and Technology*, 72, 105-118.
- DU, X., GUANG, W., CHENG, Y., HOU, Z., LIU, Z., YIN, H., HUO, L., LEI, R. & SHU, C. 2020. Thermodynamics analysis of the adsorption of CH₄ and CO₂ on montmorillonite. *Applied Clay Science*, 192, 105631.
- GAUTAM, SAH, R. P. & SAHOO, S. 2023. A review on adsorption isotherms and kinetics of CO₂ and various adsorbent pairs suitable for carbon capture and green refrigeration applications. *Sādhana*, 48, 27.

- GHATAK, M. D. & MAHANTA, P. 2016. Biogas purification using chemical absorption. *International journal of engineering and technology*, 8, 1600-1605.
- GIELEN, D., BOSHELL, F., SAYGIN, D., BAZILIAN, M. D., WAGNER, N. & GORINI, R. 2019. The role of renewable energy in the global energy transformation. *Energy strategy reviews*, 24, 38-50.
- GKOTSIS, P., KOUGIAS, P., MITRAKAS, M. & ZOUBOULIS, A. 2023. Biogas upgrading technologies—Recent advances in membrane-based processes. *International Journal of Hydrogen Energy*, 48, 3965-3993.
- GOGELA, U., SALIE, Y., PINEO, C. & BASSON, L. 2017. The business case for biogas from solid waste in the Western Cape. *GreenCape: Cape Town, South Africa*.
- HAO, P., SHI, Y., LI, S., ZHU, X. & CAI, N. 2018. Adsorbent characteristic regulation and performance optimization for pressure swing adsorption via temperature elevation. *Energy & fuels*, 33, 1767-1773.
- HASHEMIFARD, S., ISMAIL, A. F. & MATSUURA, T. 2011. Effects of montmorillonite nano-clay fillers on PEI mixed matrix membrane for CO₂ removal. *Chemical Engineering Journal*, 170, 316-325.
- INGO, C., TUUF, J. & BJÖRKLUND-SÄNKIAHO, M. 2022. Impact of hydrogen on natural gas compositions to meet engine gas quality requirements. *Energies*, 15, 7990.
- ISMAIL, A. F., KHULBE, K. C. & MATSUURA, T. 2015. Gas separation membranes. *Switz. Springer*, 10, 973-978.
- JANZEN, R., DAVIS, M. & KUMAR, A. 2020. Greenhouse gas emission abatement potential and associated costs of integrating renewable and low carbon energy technologies into the Canadian oil sands. *Journal of cleaner production*, 272, 122820.
- JI, G. & ZHAO, M. 2017. Membrane separation technology in carbon capture. *Recent advances in carbon capture and storage*, 59-90.
- KAPOOR, R., SUBBARAO, P., VIJAY, V. K., SHAH, G., SAHOTA, S., SINGH, D. & VERMA, M. 2017. Factors affecting methane loss from a water scrubbing based biogas upgrading system. *Applied Energy*, 208, 1379-1388.
- KARNE, H., MAHAJAN, U., KETKAR, U., KOHADE, A., KHADILKAR, P. & MISHRA, A. 2023. A review on biogas upgradation systems. *Materials Today: Proceedings*, 72, 775-786.
- KAUR, H., SOHPAL, V. K. & KUMAR, S. 2017. Designing of small scale fixed dome biogas digester for paddy straw. *International Journal of Renewable Energy Research*, 7, 422-31.
- KHAJURIA, H. 2011. *Model-based design, operation and control of pressure swing adsorption systems*. Department of Chemical Engineering and Chemical Technology, Imperial College

- KIHOMBO, S., AHMED, Z., CHEN, S., ADEBAYO, T. S. & KIRIKKALELI, D. 2021. Linking financial development, economic growth, and ecological footprint: what is the role of technological innovation? *Environmental Science and Pollution Research*, 28, 61235-61245.
- KONIUSZEWSKA, I., HARNISZ, M., KORZENIEWSKA, E., CZATZKOWSKA, M., JASTRZĘBSKI, J. P., PAUKSZTO, Ł., BAJKACZ, S., FELIS, E. & RUSANÓWSKA, P. 2021. The effect of antibiotics on mesophilic anaerobic digestion process of cattle manure. *Energies*, 14, 1125.
- KONIUSZEWSKA, I., KORZENIEWSKA, E., HARNISZ, M. & CZATZKOWSKA, M. 2020. Intensification of biogas production using various technologies: A review. *International Journal of Energy Research*, 44, 6240-6258.
- LÄNTELÄ, J., RASI, S., LEHTINEN, J. & RINTALA, J. 2012. Landfill gas upgrading with pilot-scale water scrubber: Performance assessment with absorption water recycling. *Applied energy*, 92, 307-314.
- LASICH, M. 2020. Upgrading wood gas using bentonite clay: a multiscale modeling and simulation study. *ACS omega*, 5, 11068-11074.
- LI, J.-R., MA, Y., MCCARTHY, M. C., SCULLEY, J., YU, J., JEONG, H.-K., BALBUENA, P. B. & ZHOU, H.-C. 2011. Carbon dioxide capture-related gas adsorption and separation in metal-organic frameworks. *Coordination Chemistry Reviews*, 255, 1791-1823.
- MALLOUPPAS, G., YFANTIS, E. A., IOANNOU, C., PARADEISIOTIS, A. & KTORIS, A. 2023. Application of Biogas and Biomethane as Maritime Fuels: A Review of Research, Technology Development, Innovation Proposals, and Market Potentials. *Energies*, 16, 2066.
- MANIARASU, R., RATHORE, S. K. & MURUGAN, S. 2023. A review on materials and processes for carbon dioxide separation and capture. *Energy & Environment*, 34, 3-57.
- MEEGODA, J. N., LI, B., PATEL, K. & WANG, L. B. 2018. A review of the processes, parameters, and optimization of anaerobic digestion. *International journal of environmental research and public health*, 15, 2224.
- MILANZI, A. N. J. 2022. *Carbon Tax Act 15 of 2019 and Its Practical Implications on the South African Mining Sector*. University of Pretoria (South Africa).
- MOHANAKRISHNAN, L., KURIAN, J. & RINTALA, J. 2016. Chemical scrubbing for removal of CO₂ from biogas using algae and H₂S using sponge iron. *International Journal of Renewable Energy and Environmental Engineering*, 4, 35-41.
- MONDAL, M. A. H., BRYAN, E., RINGLER, C., MEKONNEN, D. & ROSEGRANT, M. 2018. Ethiopian energy status and demand scenarios: prospects to improve energy efficiency and mitigate GHG emissions. *Energy*, 149, 161-172.

- MSIBI, S. S. & KORNELIUS, G. 2017. Potential for domestic biogas as household energy supply in South Africa. *Journal of Energy in Southern Africa*, 28, 1-13.
- MUTUNGWAZI, A., MUKUMBA, P. & MAKAKA, G. 2018. Biogas digester types installed in South Africa: A review. *Renewable and Sustainable Energy Reviews*, 81, 172-180.
- NAQUASH, A., QYYUM, M. A., HAIDER, J., BOKHARI, A., LIM, H. & LEE, M. 2022. State-of-the-art assessment of cryogenic technologies for biogas upgrading: Energy, economic, and environmental perspectives. *Renewable and Sustainable Energy Reviews*, 154, 111826.
- RAFIEE, A., KHALILPOUR, K. R., PREST, J. & SKRYABIN, I. 2021. Biogas as an energy vector. *Biomass and Bioenergy*, 144, 105935.
- RAGANATI, F., MICCIO, F. & AMMENDOLA, P. 2021. Adsorption of carbon dioxide for post-combustion capture: a review. *energy & fuels*, 35, 12845-12868.
- S., D. A. A.-V. R.-L. C. A. J. R. O.-G. J. R. T.-S. J. G.-R. 2010. Purification and upgrading of biogas by pressure swing adsorption on synthetic and natural zeolites. *Microporous and Mesoporous Materials*, 134, 100-107.
- SAADI, R., SAADI, Z., FAZAELI, R. & FARD, N. E. 2015. Monolayer and multilayer adsorption isotherm models for sorption from aqueous media. *Korean Journal of Chemical Engineering*, 32, 787-799.
- SAUTETJ, D. L., STRAHLK, S., SERRAK, M., POLVERINOL, P., PIANESEL, C., MAYURM, M., BESSLERM, W. & KOMPISN, C. Performance and degradation of Proton Exchange Membrane Fuel Cells: State of the art in modeling from atomistic to system scale.
- SCARLAT, N., DALLEMAND, J.-F. & FAHL, F. 2018. Biogas: Developments and perspectives in Europe. *Renewable energy*, 129, 457-472.
- SRIVASTAVA, R. K., SHETTI, N. P., REDDY, K. R. & AMINABHAVI, T. M. 2020. Sustainable energy from waste organic matters via efficient microbial processes. *science of the total environment*, 722, 137927.
- TAO, Y., ZHANG, G. & XU, H. 2022. Grand canonical Monte Carlo (GCMC) study on adsorption performance of metal organic frameworks (MOFs) for carbon capture. *Sustainable Materials and Technologies*, 32, e00383.
- THOPI, M. S., BANSAL, R. C., ZHANG, L. & SHARMA, G. 2018. A review of grid connected distributed generation using renewable energy sources in South Africa. *Energy strategy reviews*, 21, 88-97.
- UPADHYAY, A., KOVALEV, A. A., ZHURAVLEVA, E. A., KOVALEV, D. A., LITTI, Y. V., MASAKAPALLI, S. K., PAREEK, N. & VIVEKANAND, V. 2022. Recent development in physical, chemical, biological and hybrid biogas upgradation techniques. *Sustainability*, 15, 476.

- XIAO, Z., BI, C., SHAO, Y., DONG, Q., WANG, Q., YUAN, Y., WANG, C., GAO, Y. & HUANG, J. 2014. Efficient, high yield perovskite photovoltaic devices grown by interdiffusion of solution-processed precursor stacking layers. *Energy & Environmental Science*, 7, 2619-2623.
- YOUSEF, A. M., EL-MAGHLANY, W. M., ELDRAINNY, Y. A. & ATTIA, A. 2018. New approach for biogas purification using cryogenic separation and distillation process for CO₂ capture. *Energy*, 156, 328-351.
- YUAN, T., ZHANG, Z., LEI, Z., SHIMIZU, K. & LEE, D.-J. 2022. A review on biogas upgrading in anaerobic digestion systems treating organic solids and wastewaters via biogas recirculation. *Bioresource Technology*, 344, 126412.
- YUSUF, N. & ALMOMANI, F. 2023. Recent advances in biogas purifying technologies: Process design and economic considerations. *Energy*, 265, 126163.
- ZHOU, K., CHAEMCHUEN, S. & VERPOORT, F. 2017. Alternative materials in technologies for Biogas upgrading via CO₂ capture. *Renewable and sustainable energy reviews*, 79, 1414-1441.

APPENDIX A: SIMULATION DETAILS AND CALCULATIONS

T= 298K

P= 0.01 – 1000 kPa

Mass of Adsorbent = 4468g

Average = \sum isotherm/Madsorbent

$$= \frac{\sum(4.5 \times 10^{-6} + 5.10 \times 10^{-6} + 5.05 \times 10^{-6})}{4468} = 1.09 \times 10^{-3} \text{ mol/g}$$

Standard deviation = Stdv(\sum isotherm)/ M_{adsorbent}

$$= \frac{STDV(\sum 4.50^{-6} + 5.10 \times 10^{-6} + 5.05 \times 10^{-6})}{4468} = 7.45 \times 10^{-11} \text{ mol/g}$$

Table A-1 Present calculations pf standard deviation

f(KPa)(N₂)	P(kPa)	1st Simulation	2nd Simulation	3rd Simulation	Average	Standard deviation
1.0 x10 ⁻³	1.0 x10 ⁻³	4.50 x10 ⁻⁶	5.10 x10 ⁻⁶	5.05 x10 ⁻⁶	1.09 x10 ⁻⁹	7.45 x10 ⁻¹¹
1.47 x10 ⁻²	1.47 x10 ⁻²	8.61 x10 ⁻⁵	7.59 x10 ⁻⁵	8.83 x10 ⁻⁵	1.87 x10 ⁻⁸	1.48 x10 ⁻⁹
2.15 x10 ⁻¹	2.15 x10 ⁻¹	1.28 x10 ⁻³	1.29 x10 ⁻³	1.26 x10 ⁻³	2.86 x10 ⁻⁷	3.66 x10 ⁻⁹
3.16	3.16	1.88 x10 ⁻²	1.88 x10 ⁻²	1.89 x10 ⁻²	4.22 x10 ⁻⁶	2.55 x10 ⁻⁹
4.64 x10 ¹	4.63 x10 ¹	2.76 x10 ⁻¹	2.75 x10 ⁻¹	2.75 x10 ⁻¹	6.16 x10 ⁻⁵	1.58 x10 ⁻⁷
6.81 x10 ²	6.84 x10 ²	3.61	3.60	3.60	8.07 x10 ⁻⁴	1.42 x10 ⁻⁶
1 x10 ³	1.03 x10 ⁴	2.16 x10 ¹	2.17 x10 ¹	2.17 x10 ¹	4.85 x10 ⁻³	9.92 x10 ⁻⁶

Table A-2 Present calculations pf standard deviation

f(KPa)(CH₄)	P(kPa)	1st	2nd	3rd	Average	Standard
		Simulation	Simulation	Simulation		deviation
1.0 x10 ⁻³	1.0 x10 ⁻³	5.91 x10 ⁻⁵	5.82 x10 ⁻⁵	5.64 x10 ⁻⁵	1.29 x10 ⁻⁸	3.02 x10 ⁻¹⁰
1.47 x10 ⁻²	1.47 x10 ⁻²	8.39 x10 ⁻⁴	8.38 x10 ⁻⁴	8.18 x10 ⁻⁴	1.86 x10 ⁻⁷	2.72 x10 ⁻⁹
2.15 x10 ⁻¹	2.15 x10 ⁻¹	1.21 x10 ⁻²	1.20 x10 ⁻²	122 x10 ⁻²	2.71 x10 ⁻⁶	1.64 x10 ⁻⁸
3.16	3.16	1.79 x10 ⁻¹	1.77 x10 ⁻¹	1.76 x10 ⁻¹	3.95 x10 ⁻⁵	9.27 x10 ⁻⁸
8.52 x10 ¹	8.65 x10 ¹	2.49	2.49	2.48	5.57 x10 ⁻⁴	1.64 x10 ⁻⁶
6.81 x10 ²	6.94 x10 ²	2.01 x10 ¹	2.02 x10 ¹	2.02 x10 ¹	4.51 x10 ⁻³	1.26 x10 ⁻⁵
1 x10 ³	1.28 x10 ⁴	4.66 x10 ¹	4.67 x10 ¹	4.66 x10 ¹	1.04 x10 ⁻²	1.45 x10 ⁻⁵

Table A-3 Present calculations pf standard deviation

f(KPa)	P (kPa)	1st	2nd	3rd	Average	Standard
C₂H₆		Simulation	Simulation	Simulation		deviation
1.0 x10 ⁻³	1.0 x10 ⁻³	7.53 x10 ⁻⁴	7.8 x10 ⁻⁴	7.80 x10 ⁻⁴	1.73 x10 ⁻⁷	3.49 x10 ⁻⁹
1.47 x10 ⁻²	1.47 x10 ⁻²	1.13 x10 ⁻²	1.14 x10 ⁻²	1.13 x10 ⁻²	2.53 x10 ⁻⁶	1.11 x10 ⁻⁸
2.15 x10 ⁻¹	2.15 x10 ⁻¹	1.68 x10 ⁻¹	1.67 x10 ⁻¹	1.66 x10 ⁻¹	3.74 x10 ⁻⁵	2.76 x10 ⁻⁷
3.16	3.16	2.49	2.48	2.49	5.57 x10 ⁻⁴	2.14 x10 ⁻⁶
8.52 x10 ¹	4.66 x10 ¹	1.89 x10 ¹	1.89 x10 ¹	1.89 x10 ¹	4.24 x10 ⁻³	4.32 x10 ⁻⁶
6.81 x10 ²	7.32 x10 ¹	22.65 x10 ¹	2.66 x10 ¹	2.68 x10 ¹	5.96 x10 ⁻³	3.73 x10 ⁻⁵
1 x10 ³	4.73 x10 ⁴	4.37 x10 ¹	4.54 x10 ¹	4.49 x10 ¹	9.99 x10 ⁻³	1.91 x10 ⁻⁴

Table A-4 Present calculations pf standard deviation

f(KPa) CO₂	P(kPa)	1st Simulation	2nd Simulation	3rd Simulation	Average	Standard deviation
1.0 x10 ⁻³	1.0 x10 ⁻³	2.13 x10 ⁻⁵	2.27 x10 ⁻⁵	1.88 x10 ⁻⁵	4.67 x10 ⁻⁹	4.42 x10 ⁻¹⁰
1.47 x10 ⁻²	1.47 x10 ⁻²	3.22 x10 ⁻⁴	3.28 x10 ⁻⁴	3.15 x10 ⁻⁴	7.20 x10 ⁻⁸	1.41 x10 ⁻⁹
2.15 x10 ⁻¹	2.15 x10 ⁻¹	4.80 x10 ⁻³	4.73 x10 ⁻³	4.68 x10 ⁻³	1.06 x10 ⁻⁶	1.35 x10 ⁻⁸
3.16	3.16	6.83 x10 ⁻²	6.84 x10 ⁻²	6.89 x10 ⁻²	1.53 x10 ⁻⁵	7.84 x10 ⁻⁸
4.64 x10 ¹	4.66 x10 ¹	9.80 x10 ⁻¹	9.72 x10 ⁻¹	9.85 x10 ⁻¹	2.19 x10 ⁻⁴	1.42 x10 ⁻⁶
6.81 x10 ²	7.13 x10 ²	1.0 x10 ¹	1.01 x10 ¹	9.99	2.24 x10 ⁻³	7.22 x10 ⁻⁶
1 x10 ³	4.87 x10 ⁴	2.91 x10 ¹	2.89 x10 ¹	2.91 x10 ¹	6.50 x10 ⁻³	1.82 x10 ⁻⁵

Table A-5 Present calculations pf standard deviation

f(KPa) H₂S	P(kPa)	1st Simulation	2nd Simulation	3rd Simulation	Average	Standard deviation
1.0 x10 ⁻³	1.0 x10 ⁻³	6.99 x10 ⁻⁵	6.88 x10 ⁻⁵	6.10 x10 ⁻⁵	1.49 x10 ⁻⁸	1.09 x10 ⁻⁹
1.47 x10 ⁻²	1.47 x10 ⁻²	9.29 x10 ⁻⁴	9.70 x10 ⁻⁴	9.28 x10 ⁻⁴	2.11 x10 ⁻⁷	5.25 x10 ⁻⁹
2.15 x10 ⁻¹	2.15 x10 ⁻¹	1.39 x10 ⁻²	1.37 x10 ⁻²	1.37 x10 ⁻²	3.0 x10 ⁻⁶	1.85 x10 ⁻⁸
3.16	3.16	2.02 x10 ⁻¹	2.03 x10 ⁻¹	2.02 x10 ⁻¹	4.53 x10 ⁻⁵	1.04 x10 ⁻⁷
4.64 x10 ¹	4.66 x10 ¹	2.84	2.84	2.84	6.35 x10 ⁻⁴	5.24 x10 ⁻⁷
6.81 x10 ²	7.29 x10 ²	2.11 x10 ¹	2.09 x10 ¹	2.11 x10 ¹	4.71 x10 ⁻³	1.03 x10 ⁻⁵
1 x10 ³	1.32 x10 ⁴	4.68 x10 ¹	4.62 x10 ¹	4.62 x10 ¹	1.03 x10 ⁻²	1.03 x10 ⁻⁵

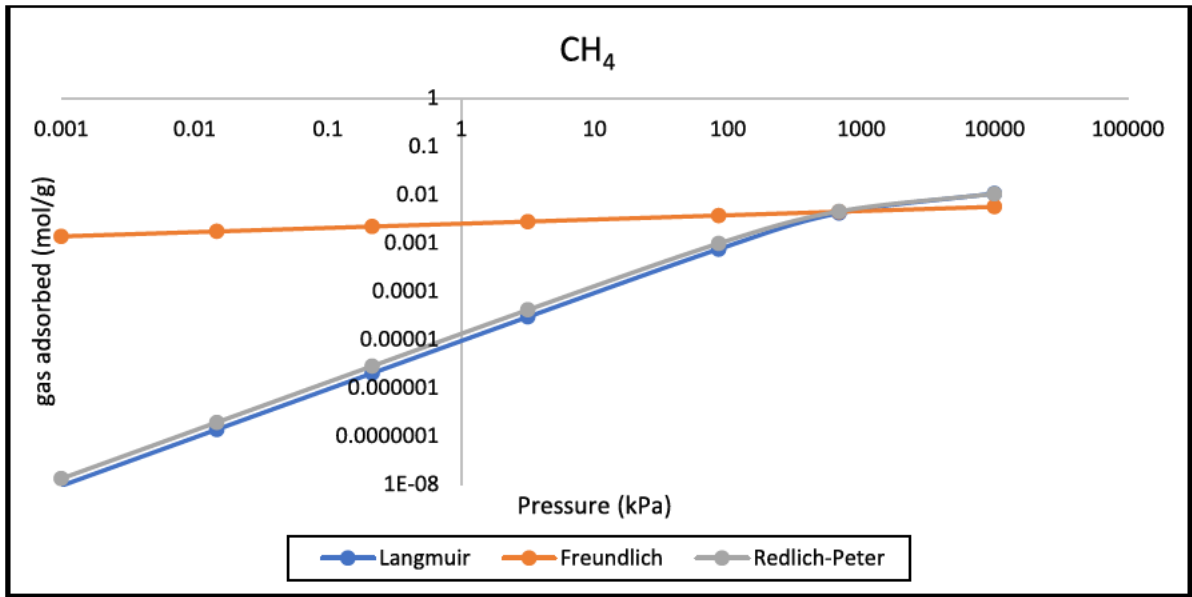


Figure A-1 The quantity of gas adsorbed into the adsorbent q , and P as the pressure.

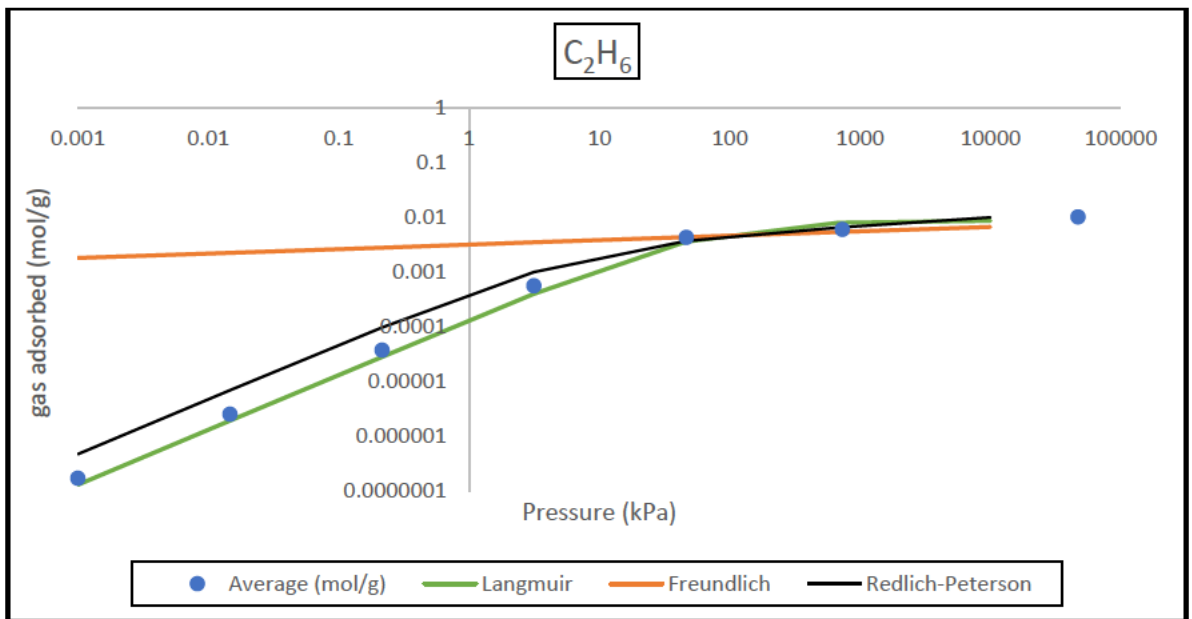


Figure A-2 The quantity of gas adsorbed into the adsorbent q , and P as the pressure.

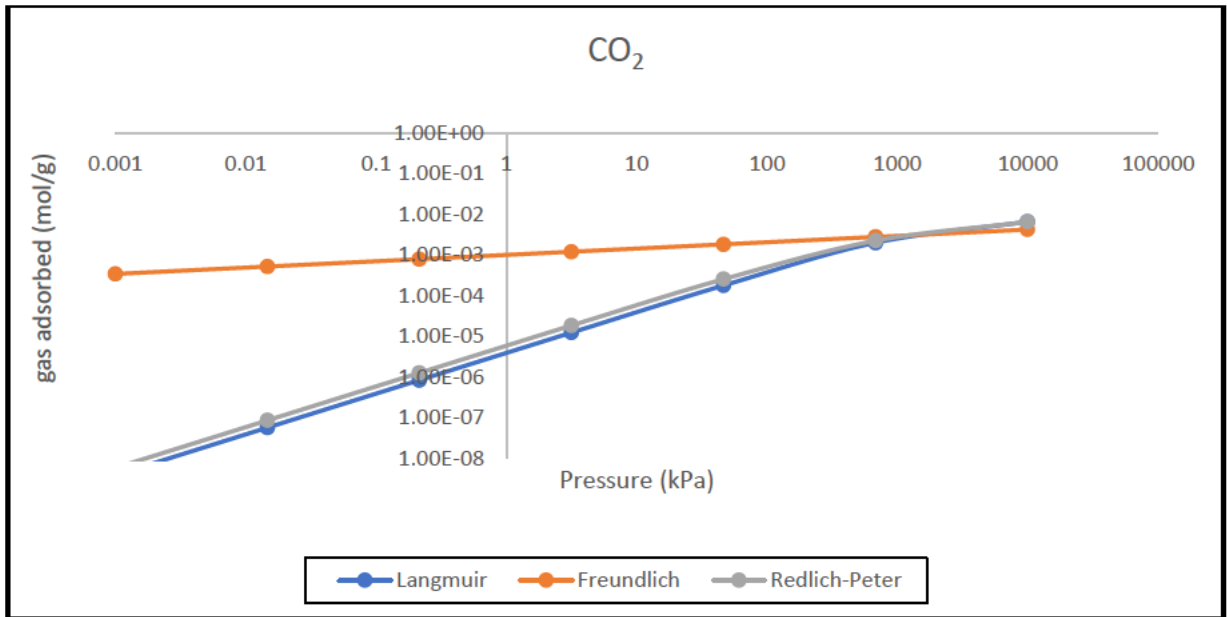


Figure A-3 The quantity of gas adsorbed into the adsorbent q , and P as the pressure.

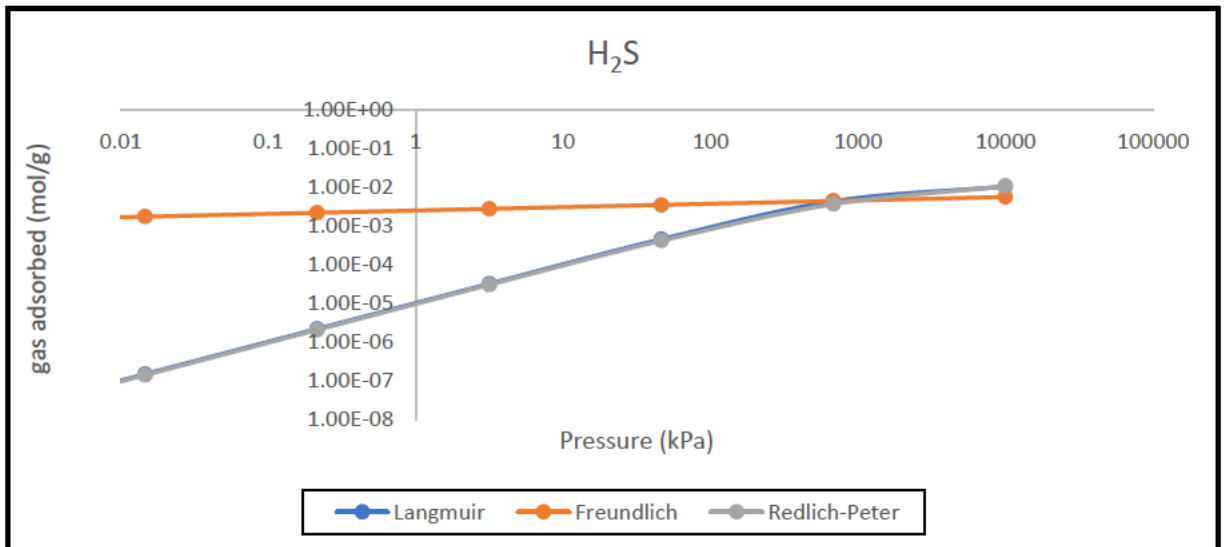


Figure A-4 The quantity of gas adsorbed into the adsorbent q , and P as the pressure.

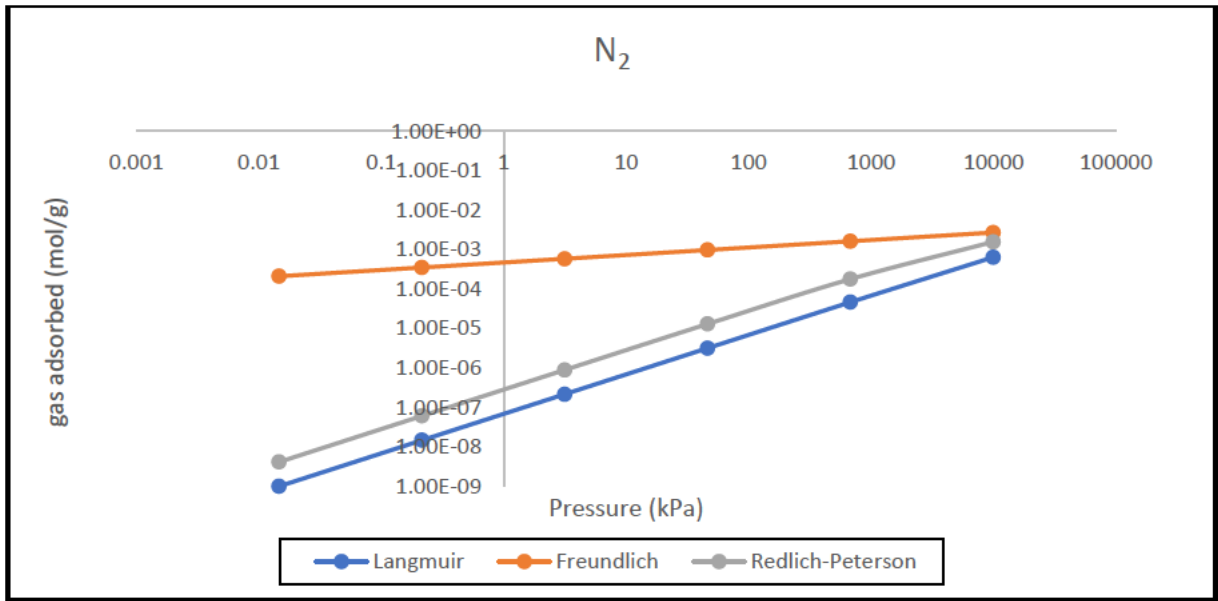


Figure A-5 The quantity of gas adsorbed into the adsorbent q , and P as the pressure.

APPENDIX B: CALCULATIONS FOR BEST FIT MODEL

B1: Comparison between Langmuir, Freundlich and Redlich -Peterson using the following equations respectively:

$$q = \frac{q_0 b P}{1 + b P} \quad \text{Equation B.1}$$

$$q = K_f \frac{1}{n} \quad \text{Equation B.2}$$

$$q = \frac{K_g P}{1 + a R P^b} \quad \text{Equation B.3}$$

Langmuir: using equation (B1.1)

$$= \frac{1.19E-2 \times 7.79E-4 \times 0.01}{1 + 7.79E-4 \times 0.01} = 9.3 \times 10^{-11}$$

Freundlich: equation (B1.2)

$$= 2.5 \times 10 \times 0.01^{1/11.41744} = 1.37 \times 10^{-3}$$

Redlich-Peterson: equation (B1.3)

$$= \frac{1.30 \times 10^{-5} \times 1.0 \times 10^{-2}}{1 + 2.44 \times 10^{-3} \times 1.0 \times 10^{-2(9.19 \times 10^{-1})}} = 1.31 \times 10^{-8}$$

Root Mean Square Error: $(q - \text{average})^2$

$$= (9.30 \times 10^{-11} - 1.29 \times 10^{-8})^2 = 1.33 \times 10^{-17}$$

Sum Squared Error: $\sum \text{RMSE} = 1.95 \times 10^{-7}$

Absolute deviation: $ABS \frac{q - \text{average}}{\text{average} \times 100}$

$$ABS = \frac{9.30 \times 10^{-7} - 1.29 \times 10^{-8}}{1.29 \times 10^{-8} \times 100} = 28.18$$

$R^2 = \text{Correlation} (\sum \text{average}; \sum q) = 0.99$

The calculations and comparison were conducted for all species and the results are presented in Table B1.1 to B1.5.

Table B-1 CH₄ Fitted Mode parameters of Langmuir, Freundlich and Redlich-Peterson along with RMSE and R²

Langmuir	Squared error	SSE	Absolute dev	R ²	Freundlich	Squared error	SSE	Absolute dev	R ²
9.30 x10 ⁻⁹	1.33 x10 ⁻¹⁷	1.95 x10 ⁻⁷	28.18	0.99	1.37 x10 ⁻³	1.86 x10 ⁻⁶	5.02 x10 ⁻⁵	1.05 x10 ⁷	0.88
1.37 x10 ⁻⁷	2.46 x10 ⁻¹⁵		26.64		1.73 x10 ⁻³	2.98 x10 ⁻⁶		9.28 x10 ⁵	
2.00 x10 ⁻⁶	4.90 x10 ⁻¹³		25.89		2.19 x10 ⁻³	4.77 x10 ⁻⁶		8.08 x10 ⁴	
2.93 x10 ⁻⁵	1.02 x10 ⁻¹⁰		25.63		2.77 x10 ⁻³	7.44 x10 ⁻⁶		6.91 x10 ³	
7.43 x10 ⁻⁴	3.47 x10 ⁻⁸		33.43		3.69 x10 ⁻³	9.82 x10 ⁻⁶		5.63 x10 ²	
4.14 x10 ⁻³	1.37 x10 ⁻⁷		8.22		4.43 x10 ⁻³	6.87 x10 ⁻⁹		1.84	
1.06 x10 ⁻²	2.27 x10 ⁻⁸		1.44		5.60 x10 ⁻³	2.34 x10 ⁻⁵		4.63 x10 ¹	
		AAD	21.35					1.65 x10 ⁶	
-	Squared error	SSE	Absolute dev	R ²	Langmuir	Q _o	b		
1.31 x10 ⁻⁸	1.22 x10 ⁻²⁰	1.73 x10 ⁻⁷	0.85	0.99		1.90 x10 ⁻²	7.79 x10 ⁻⁴		
1.92 x10 ⁻⁷	3.14 x10 ⁻¹⁷		3.01						
2.81 x10 ⁻⁶	1.18 x10 ⁻¹⁴		4.02		Freundlich	K _f	n		
4.10 x10 ⁻⁵	2.45 x10 ⁻¹²		3.97			2.50 x10 ⁻³	11.42		
9.73 x10 ⁻⁴	1.73 x10 ⁻⁷		74.56						
4.50 x10 ⁻³	6.94 x10 ⁻¹¹		0.18						
1.04 x10 ⁻²	4.65 x10 ⁻¹²		0.02		Redlich	K _g	aR		
						1.31 x10 ⁻⁵	2.44 x10 ⁻³		
		AAD	12.37		B _s	9.19 x10 ¹			

Table B-2 C₂H₆ Fitted Mode parameters of Langmuir, Freundlich and Redlich-Peterson along with RMSE and R²

Langmuir	Squared error	SSE	Absolute dev	R²	Freundlich	Squared error	SSE	Absolute dev	R²
1.31 x10 ⁻⁷	1.71 x10 ⁻¹⁵	6.13 x10 ⁻⁶	23.99	0.97	1.79 x10 ⁻³	3.23 x10 ⁻⁶	3.60 x10 ⁻⁵	1.04 x10 ⁶	0.97
1.92 x10 ⁻⁶	3.72 x10 ⁻¹³		24.07		2.23 X10 ⁻³	4.97 x10 ⁻⁶		8.79 x10 ⁴	
2.82 x10 ⁻⁵	8.57 x10 ⁻¹¹		24.74		2.77 x10 ⁻³	7.48 x10 ⁻⁶		7.3 x10 ²	
3.96 x10 ⁻⁴	2.60 x10 ⁻⁸		28.97		3.44 x10 ⁻³	8.33 x10 ⁻⁶		5.18 x10 ²	
3.6 x10 ⁻³	4.54 x10 ⁻⁷		15.89		4.28 x10 ⁻³	1.46 x10 ⁻⁹		9.00 x10 ⁻¹	
7.85 x10 ⁻³	3.56 x10 ⁻⁶		31.64		5.31 x10 ⁻³	4.25 x10 ⁻⁷		1.09 x10 ¹	
8.55 x10 ⁻³	2.09 x10 ⁻⁶		14.44		6.60 x10 ⁻³	1.15 x10E-5		3.39 x10 ¹	
		AAD	23.39					1.62 x10 ⁵	
Redlich-Peterson	Squared error	SSE	Absolute dev	R²	Langmuir	Qo	b		
4.75 x10 ⁻⁷	9.13 x10 ⁻¹⁴	7.86 x10 ⁻⁷	175.19	0.99		8.61 x10 ⁻³	1.52 x10 ⁻²		
6.93 x10 ⁻⁶	1.94 x10 ⁻¹¹		173.66						
9.72 x10 ⁻⁵	3.58 x10 ⁻⁹		159.89		Freundlich	K_f	n		
9.93 x10 ⁻⁴	1.90 x10 ⁻⁷		78.28			3.14 x10 ⁻³	12.38		
3.66 x10 ⁻³	3.34 x10 ⁻⁷		13.63						
6.45 x10 ⁻³	2.37 x10 ⁻⁷		8.16						
9.85 x10 ⁻³	2.20 x10 ⁻⁸		1.48		Redlich	K_g	aR		
						4.75 x10 ⁻⁴	0.19		
		AAD	87.18		B_s	0.85			

Table B-3 CO₂ Fitted Mode parameters of Langmuir, Freundlich and Redlich-Peterson along with RMSE and R²

Langmuir	Squared error	SSE	Absolute dev	R²	Freundlich	Squared error	SSE	Absolute dev	R2
3.93 x10 ⁻⁹	5.50 x10 ⁻¹⁹	6.70 x10 ⁻⁸	15.86	0.99	3.43 x10 ⁻⁴	1.17 x10 ⁻⁷	1.05 x10 ⁻⁵	7.33 x10 ⁶	0.93
5.77 x10 ⁻⁸	2.04 x10 ⁻¹⁶		19.84		5.21 x10 ⁻⁴	2.71 x10 ⁻⁷		7.23 x10 ⁵	
8.47 x10 ⁻⁷	4.56 x10 ⁻¹⁴		20.13		7.91 x10 ⁻⁴	6.24 x10 ⁻⁷		7.45 x10 ⁴	
1.24 x10 ⁻⁵	8.58 x10 ⁻¹²		19.09		1.20 x10 ⁻³	1.41 x10 ⁻⁶		7.73 x10 ³	
1.78 x10 ⁻⁴	1.66 x10 ⁻⁹		18.59		1.82 x10 ⁻³	2.58 x10 ⁻⁶		7.33 x10 ²	
2.00 x10 ⁻³	5.96 x10 ⁻⁸		10.87		2.77 x10 ⁻³	2.8 x10 ⁻⁷		2.36 x10 ¹	
6.57 x10 ⁻³	5.69 x10 ⁻⁹		1.16		4.21 x10 ⁻³	5.21 x10 ⁻⁶		3.51 x10 ¹	
		AAD	15.08					1.16 x10 ⁶	
Redlich-Peterson	Squared error	SSE	Absolute dev	R²	Langmuir	Qo	b		
5.92 x10 ⁻⁹	1.55 x10 ⁻¹⁸	1.4 x10 ⁻⁹	26.63	0.99		7.89 x10 ⁻³	4.50 x10 ⁻⁴		
8.69 x10 ⁻⁸	2.21 x10 ⁻¹⁶		20.63						
1.27 x10 ⁻⁶	4.56 x10 ⁻¹⁴		20.12		Freundlich	K_f	n		
1.86 x10 ⁻⁵	1.04 x10 ⁻¹¹		21.02			1.0 x10 ⁻³	6.42		
2.70 x10 ⁻⁴	1.25 x10 ⁻⁹		16.13						
2.24 x10 ⁻³	3.47 x10 ⁻¹¹		0.26						
6.51 x10 ⁻³	1.06 x10 ⁻¹⁰		0.16		Redlich	K_g	aR		
						5.92 x10 ⁻⁶	2.91 x10 ⁻³		
		AAD	14.99		B_s	8.61 x10 ⁻¹			

Table B-4 H₂S Fitted Mode parameters of Langmuir, Freundlich and Redlich-Peterson along with RMSE and R²

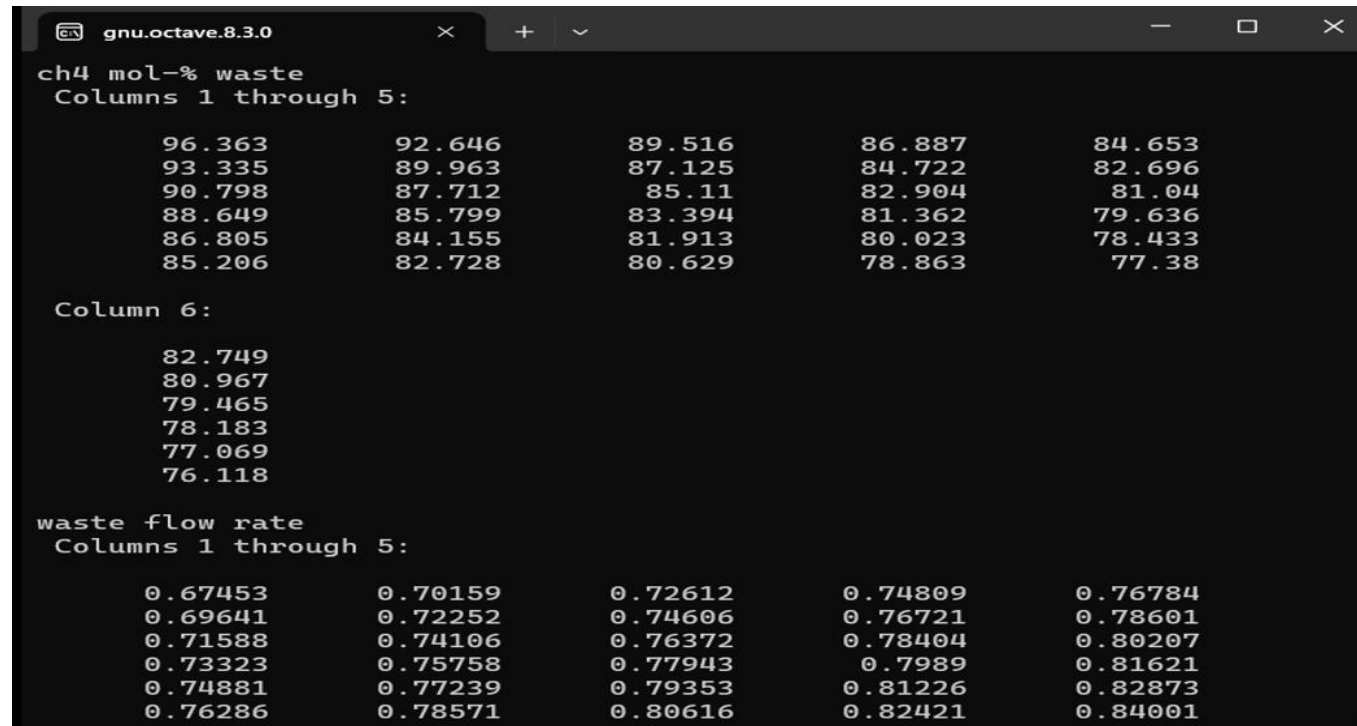
Langmuir	Squared error	SSE	Absolute dev	R²	Freundlich	Squared error	SSE	Absolute dev	R²
1.02 x10 ⁻⁸	2.21 x10 ⁻¹⁷	1.81 x10 ⁻⁷	31.57	0.99	1.38 x10 ⁻³	1.91 x10 ⁻⁶	4.78 x10 ⁻⁵	9.28 x10 ⁶	0.89
1.50 x10 ⁻⁷	3.77 x10 ⁻¹⁵		29.09		1.75 x10 ⁻³	3.05 x10 ⁻⁶		8.27 x10 ⁵	
2.19 x10 ⁻⁶	7.90 x10 ⁻¹³		28.83		2.21 x10 ⁻³	4.85 x10 ⁻⁶		7.14 x10 ⁴	
3.21 x10 ⁻⁵	1.73 x10 ⁻¹⁰		29.04		2.79 x10 ⁻³	7.52 x10 ⁻⁶		6.05 x10 ³	
4.55 x10 ⁻⁴	3.26 x10 ⁻⁸		28.43		3.52 x10 ⁻³	8.33 x10 ⁻⁶		4.54 x10 ²	
4.35 x10 ⁻³	1.24 x10 ⁻⁷		7.49		4.45 x10 ⁻³	6.61 x10 ⁻⁸		5.46	
1.05 x10 ⁻²	2.38 x10 ⁻⁸		1.49		5.62x10 ⁻³	2.21 x10 ⁻⁵		4.55 x10 ¹	
		AAD	22.28					1.45 x10 ⁶	
Redlich-Peterson	Squared error	SSE	Absolute dev	R²	Langmuir	Q_o	b		
9.72 x10 ⁻⁹	2.67 x10 ⁻¹⁷	1.24 x10 ⁻⁶	34.69	0.99		1.17 x10 ⁻²	8.72 x10 ⁻⁴		
1.43 x10 ⁻⁷	4.65 x10 ⁻¹⁵		32.34						
2.09 x10 ⁻⁶	9.81 x10 ⁻¹³		32.12		Freundlich	K_f	n		
3.05 x10 ⁻⁵	2.18 x10 ⁻¹⁰		32.62			2.52 x10 ⁻³	11.48		
4.18 x10 ⁻⁴	4.71 x10 ⁻⁸		34.15						
3.68 x10 ⁻³	1.06 x10 ⁻⁶		21.87						
1.07 x10 ⁻²	1.32 x10 ⁻⁷		3.51		Redlich	K_g	aR		
						9.72 x10 ⁻⁶	2.91 x10 ⁻³		
		AAD	27.33		B_s	0.86			

Table B-5 N₂ Fitted Mode parameters of Langmuir, Freundlich and Redlich-Peterson along with RMSE and R²

Langmuir	Squared error	SSE	Absolute dev	R²	Freundlich	Squared error	SSE	Absolute dev	R²
1.01 x10 ⁻⁹	7.05 x10 ⁻²¹	2.84 x10 ⁻⁸	7.68	0.99	2.11 x10 ⁻⁴	4.47 x10 ⁻⁸	7.46 x10 ⁻⁶	1.94 x10 ⁷	0.90
1.48 x10 ⁻⁸	1.49 x10 ⁻¹⁷		20.66		3.52 x10 ⁻⁴	1.24 x10 ⁻⁷		1.89 x10 ⁶	
2.17 x10 ⁻⁷	4.68 x10 ⁻¹⁵		23.94		5.86 x10 ⁻⁴	3.43 x10 ⁻⁷		2.05 x10 ⁵	
3.19 x10 ⁻⁶	1.06 x10 ⁻¹²		24.43		9.77 x10 ⁻⁴	9.45 x10 ⁻⁷		2.30 x10 ⁴	
4.66 x10 ⁻⁵	2.25 10 ⁻¹⁰		24.34		1.63 x10 ⁻³	2.45 x10 ⁻⁶		2.54 x10 ³	
6.41 x10 ⁻⁴	2.77 x10 ⁻⁸		20.62		2.71 x10 ⁻³	3.62 x10 ⁻⁶		2.36 x10 ²	
487 x10 ⁻³	4.86 x10 ⁻¹⁰		0.45		4.51 x10 ⁻³	1.13 x10 ⁻⁷		6.95	
		AAD	17.45					3.07 x10 ⁶	
Redlich-Peterson	Squared error	SSE	Absolute dev	R²	Langmuir	Q₀	b		
4.17 x10 ⁻⁹	9.45 x10 ⁻¹⁸	6.77 x10 ⁻⁷	2.81 x10 ²	0.98		1.07 x10 ⁻⁴	9.42 x10 ⁻³		
6.11 x10 ⁻⁸	1.80 x10 ⁻¹⁵		2.28 x10 ²						
8.97 x10 ⁻⁷	3.73 x10 ⁻¹³		2.14 x10 ²		Freundlich	K_f	n		
1.31 x10 ⁻⁵	7.84 x10 ⁻¹¹		2.09 x10 ²			7.85 x10 ⁻⁴	5.27		
1.79 x10 ⁻⁴	1.38 x10 ⁻⁸		1.91 x10 ²						
1.58 x10 ⁻³	5.91 x10 ⁻⁷		9.52 x10 ¹						
4.58 x10 ⁻³	7.24 x10 ⁻⁸		5.55		Redlich	K_g	aR		
						4.17 x10 ⁻⁶	2.91 x10 ⁻³		
		AAD	1.75 x10 ²		B_s	8.61 x10 ⁻¹			

APPENDIX C: OPERATING CONDITIONS FOR PSA SYSTEM

C.1. Best Operating Condition for PSA System



```
gnu.octave.8.3.0
ch4 mol-% waste
Columns 1 through 5:

    96.363    92.646    89.516    86.887    84.653
    93.335    89.963    87.125    84.722    82.696
    90.798    87.712    85.11    82.904    81.04
    88.649    85.799    83.394    81.362    79.636
    86.805    84.155    81.913    80.023    78.433
    85.206    82.728    80.629    78.863    77.38

Column 6:

    82.749
    80.967
    79.465
    78.183
    77.069
    76.118

waste flow rate
Columns 1 through 5:

    0.67453    0.70159    0.72612    0.74809    0.76784
    0.69641    0.72252    0.74606    0.76721    0.78601
    0.71588    0.74106    0.76372    0.78404    0.80207
    0.73323    0.75758    0.77943    0.7989    0.81621
    0.74881    0.77239    0.79353    0.81226    0.82873
    0.76286    0.78571    0.80616    0.82421    0.84001
```

Figure C-1 Generated results obtained for PSA system using Octave tool.

Calculations for the inlet stream

Table C-1 Number of moles for the inlet stream

Assume ideal gas	CH ₄	C ₂ H ₆	CO ₂	H ₂ S	N ₂
PV= nRT	0.65	0.1	0.05	0.05	0.15
n _{feed}	9.83 x10 ⁻³	3.63 x10 ⁻²	3.74 x10 ⁻²	1.01 x10 ⁻²	7.89 x10 ⁻³

Table C-2 Number of moles for the inlet stream

Octave results	CH ₄	C ₂ H ₆	H ₂ S	N ₂	CO ₂
Composition	0.96	1.70 x10 ⁻²	1.30 x10 ⁻²	1.00 x10 ⁻²	1
n=cv	1.82 x10 ⁻³	3.23 x10 ⁻⁵	2.47 x10 ⁻⁴	1.91 x10 ⁻⁵	1.90 x10 ⁻³
b	7.79 x10 ⁻⁴	1.52 x10 ⁻²	8.72 x10 ⁻⁴	1.07 x10 ⁻⁴	4.99 x10 ⁻⁴
Qo	1.19 x10 ⁻³	8.61 x10 ⁻³	1.17 x10 ⁻²	9.42 x10 ⁻³	7.89 x10 ⁻³

Bed mass calculations for CH₄: The calculations were performed at different points of the operating pressure from the PSA system.

$$W = (n_f - n_{out}) \frac{1+bp}{qbp}$$

Equation C.1

Table C-3 Bed size for CH₄ outlet stream

P(kPa) CH ₄	W(g/mol)
1 x10 ⁻³	5.24 x10 ⁻⁷
1.45 x10 ⁻²	7.69 x10 ⁻⁶
2.15 x10 ⁻¹	1.14 x10 ⁻⁴
3.16	1.66 x10 ⁻³
4.65 x10 ¹	2.45 x10 ⁻²
6.94 x10 ³	3.92 x10 ⁻¹
1.28 x10 ⁴	8.10

Best operating conditions for PSA system

Pressure: 70-80kPa

Temperature: 298K

Bed mass: 30.39g/mol.

CH₄ purity: 96%

$$\text{Separation factor} : \frac{\frac{C_{ch4_{in}}}{C_{ch4_{out}}}}{\frac{C_{co2}}{C_{ch4_{out}}}} = \frac{0.65/0.96}{0.05/0.96} = 13$$